CHAPTER

4

Elementary Particles

4.1. ***Fundamental properties of elementary particles.*** Elementary particles are characterized by the following parameters: mass, spin, electric charge, magnetic moment.

The *mass* is best defined as the constant, m, that enters in the relations between the total energy, U, the momentum, p, and the velocity, βc, of the particle, such as $U = mc^2/\sqrt{1-\beta^2}$, $U^2 = p^2c^2 + m^2c^4$, etc. A simultaneous measurement of two of the above quantities, therefore, yields the value of the mass.

The *spin* represents an intrinsic angular momentum of the particle. The natural unit for the spin is $\hbar = h/2\pi$, the angular momentum of a point mass moving along an orbit with azimuthal quantum number one. In terms of $\hbar$, the spins of elementary particles are represented by integer or half-integer numbers. The value of the spin determines the number of possible orientations of a particle with respect to a predetermined direction; for a particle of spin s this number is $2s + 1$.* Elementary particles with half-integer spin obey Pauli's exclusion principle, whereas particles with integer spin do not. Therefore the average behavior of a large number of identical particles with half-integer spin is described by Fermi's statistics; that of particles with integer spin is described by Bose's statistics.

The *electric charge* and the *magnetic moment* determine the effects of an electromagnetic field upon the particle. Thus, in the frame of reference where the particle is at rest, the product of the electric charge and the electric field intensity gives the force acting upon the particle, whereas the product of the magnetic moment, the magnetic field intensity, and the sine of the angle between the two gives the torque. The natural unit for the electric charge is the charge, e, of the electron (§ 4.3). The natural unit for the magnetic moment of a particle of charge e and mass m is $e\hbar/2mc$. This represents the orbital magnetic moment of the particle under consideration in a quantum state with azimuthal quantum number one. The quantity, $e\hbar/2m_ec$, where m_e is the electron mass, is called the

* Photons represent an exception to this rule because their spin is 1 and yet they have only two possible orientations (see § 4.2). This anomalous behavior is connected with the fact that their mass is zero.

Bohr magneton. The quantity, $e\hbar/2M_pc$, where M_p is the proton mass, is called the *nuclear magneton.*

In the transformations of elementary particles as well as in the interactions of elementary particles between themselves and with atoms, the total electric charge, the total energy, the total momentum, and the total angular momentum are conserved. Since the orbital angular momentum of a system is always an integer multiple of $\hbar$, it follows from the conservation of angular momentum that no reaction can change the number of particles with half-integer spin from odd to even or vice versa. This, of course, does not imply that the resultant spin moment is conserved, because the spin of any one particle can flip during an interaction, or two particles with spin $\frac{1}{2}$ may give rise to a particle of spin zero.

The parameters listed above do not describe the properties of elementary particles completely because elementary particles may interact with one another through forces of non-electromagnetic character, the so-called *nuclear forces*. It has not been possible as yet to describe nuclear forces completely by means of one or several parameters.

4.2. ***Photons.*** Photons, or γ-rays, considered as elementary particles, have zero mass, as shown by the fact that their velocity is always equal to c and their energy to c times their momentum. Photons have integer spin, because they are emitted in transitions between quantum states of atoms in which the angular momentum changes by an integer multiple of $\hbar$. Photons obey Bose's statistics, as shown by the fact that application of Bose's statistics to photons in thermodynamic equilibrium yields the correct expression for the spectrum of the black-body radiation (Planck's law). The assumption that the spin of photons is 1 is in agreement with the selection rules for radiative transitions. A photon in a state of definite spin orientation corresponds to a circularly polarized wave. The spin may be either parallel or anti-parallel to the direction of motion and has therefore only two possible orientations, as pointed out in § 4.1.

Photons have no electric charge and no magnetic moment.

4.3. ***Negative and positive electrons.*** Negative electrons (negatons) are among the constituents of ordinary matter. Their electric charge is accurately known (for instance, from oil-drop experiments) and has the value $e = 4.802 \cdot 10^{-10}$ e.s.u. Their mass is also accurately known (for instance, from deflection experiments in electric and magnetic fields yielding the ratio of the electric charge to the mass) and has the value $m_e = 9.105 \cdot 10^{-28}$ g. The corresponding value of the rest energy is $m_ec^2 = 0.51079$ Mev. Analysis of atomic spectra shows that the spin of negative electrons is $s = \frac{1}{2}$ and that their magnetic moment equals one Bohr magneton ($e\hbar/2m_ec$). Because of their half-integer spin, negative electrons obey Fermi's statistics. This is in agreement with experimental data on the atomic structure and on the behavior of electrons in metals.

Positive electrons (positons) do not exist in matter because as soon as they are slowed down, they undergo annihilation by combining with negative electrons. In this process, which may be regarded as the inverse of pair production, the positive and the negative electrons disappear and their energy is converted into photons. The annihilation of the two electrons gives rise, in most cases, to two photons, more rarely to a single photon. One-photon annihilation can occur only if the negative electron is tightly bound to a nucleus, as the participation of the nucleus into the process is necessary for the conservation of momentum. Two-photon annihilation may occur instead if the negative electron is free. Often the annihilation process takes place after the positon has practically come to rest. In this case the two photons are emitted in opposite directions with equal energies.

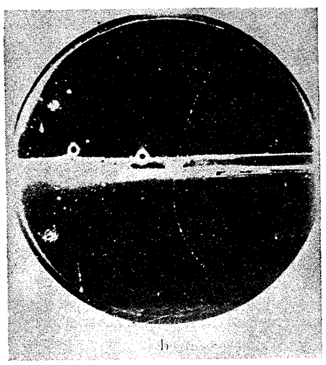

Fig. 4.3.1. Cloud-chamber picture of a positive electron. From Anderson (ACD33).

Positive electrons were discovered by Anderson (ACD32; ACD33) in the course of cloud-chamber experiments on cosmic rays. Figure 1 is the reproduction of a cloud-chamber picture obtained by Anderson. It shows a positive particle entering a 0.6-cm lead plate with a momentum of $6.3 \cdot 10^7$ ev/c and emerging with a momentum of $2.3 \cdot 10^7$ ev/c. One can set an upper limit to the mass of this particle by assuming that it loses energy only by collision. This limit is $20m_e$. From the evidence provided by this and by other similar photographs, Anderson tentatively asserted the existence of positive particles with mass nearly equal to that of ordinary electrons. This conclusion was soon confirmed by cloud-chamber observations of Blackett and Occhialini (BPM33). Shortly afterwards Curie and Joliot found that positive electrons can be generated by

materialization of γ-rays from radioactive sources (CI33.1) and are also emitted by artificially produced radioactive isotopes (CI33.2).

Since materialization of a neutral photon gives rise to a positive and a negative electron, the principle of conservation of electric charge insures that the charge of positive electrons is, in absolute value, identical to that of negative electrons.

The first quantitative determination of the mass of the positive electrons was made by Thibaud (TJ34), who measured the ratio e/m by the trochoid method and concluded that the masses of positive and negative electrons could not differ by more than 15 per cent. Later experiments by Spees and Zahn (SpA40) by means of a mass-spectrographic arrangement showed that the two masses are the same within 2 per cent. More recently DuMond and his collaborators (DMJ49.1) measured very accurately the wave length of the annihilation radiation. Within the experimental error of the measurement (0.2 per cent) they found the value predicted under the assumption that positive and negative electrons have identical masses.

Conservation of angular momentum, applied to the pair-production process, shows that positive electrons have half-integer spin and obey, therefore, Fermi's statistics. It is reasonable to assume that their spin is $\frac{1}{2}$ as is that of negative electrons.

4.4. *Protons and neutrons.* Protons and neutrons are the constituents of atomic nuclei and are therefore often referred to as *nucleons*. Neutrons have no electric charge. Protons have a positive electric charge equal in magnitude to the charge of electrons. This is shown by the fact that atoms are neutral. The proton mass, M_p, is accurately known from direct mass-spectographic determinations. Its value is 1836 times the electron mass. The corresponding rest energy is 938 Mev. The mass of neutrons, M_n, is known from mass-spectrographic determination of the mass of the deuteron (which is formed by one proton and one neutron) and from the measurement of the binding energy of this particle. Its value is slightly greater than that of the proton mass. The corresponding difference in rest energy is about 1.3 Mev.

The hyperfine structure of hydrogen shows that the proton has spin $\frac{1}{2}$. The hyperfine structure of deuterium shows that the deuteron has spin 1. Therefore the neutron must have half-integer spin and it is natural to assume that it has spin $\frac{1}{2}$. This assumption is confirmed in a very direct way by experimental data on the scattering of slow neutrons by ortho- and para-hydrogen (SwJ40; SRB47).

The magnetic moments of the proton and the neutron have been determined by magnetic resonance methods; i.e., by means of experiments in which one measures the energy difference for a particle oriented either parallel or antiparallel to a magnetic field (KJM39; AWR46; the quantity actually measured is the frequency corresponding to this energy difference). The values thus found were:

for the proton: 2.7896 nuclear magnetons;

for the neutron: -1.9103 nuclear magnetons.

The minus sign for the magnetic moment of neutrons means that the magnetic moment and the spin have opposite directions. That protons and neutrons have magnetic moments of opposite sign was first shown by the finding that the deuteron has a spin equal to the sum of the spins of the proton and the neutron but has a magnetic moment approximately equal to the difference between the magnetic moments of the two particles. The signs of the magnetic moments of the proton and the neutron were later determined directly by Rogers and Staub (REH49).

4.5. *The beta decay and the neutrino.* It has been known for a long time that nuclei can emit positive or negative electrons (β-activity). One interprets this phenomenon by assuming that one of the protons of the nucleus changes into a neutron and produces a positive electron or that one of the neutrons in the nucleus changes into a proton and produces a negative electron. Outside of a nucleus, only the transformation of a neutron into a proton is energetically possible, as the rest energy of the neutron is larger than that of the proton. Such transformation has been observed (SAH50; RJM51), and the mean life of free neutrons seems to be approximately 13 minutes (RJM51).

Since protons, neutrons, and electrons have spin $\frac{1}{2}$, conservation of angular momentum rules out the possibility that an electron and a proton are the only products of the disintegration of a free neutron, or that, in the β-decay, only one electron is emitted by a nucleus. Moreover, it has been shown that the electrons emitted in the β-decay of a given radioactive isotope have a continuous energy distribution. The maximum electron energy corresponds to the difference in binding energy of the parent and daughter substances, but the average electron energy is considerably smaller than this difference. Thus, the principles of conservation of energy and of angular momentum require the existence of a neutral particle of half-integer spin, which is produced simultaneously with the electron in the β-decay and which carries the balance of the energy released in this process. This particle is called the "neutrino."

If we indicate protons, neutrons, electrons, and neutrinos by the symbols p, n, e, and ν respectively, the disintegration of a neutron is represented by the equation:

$$n \to p + e + \nu. \quad (1)$$

The mass of the neutrino is known to be less than 2 per cent of the electron mass (HCC49). Its spin is supposed to be $\frac{1}{2}$. The interactions of neutrinos with matter are very weak, as shown by the fact that no such interactions have been detected so far. This means that the magnetic moment of the neutrino is probably zero, certainly very small compared with the Bohr magneton.

4.6. *The discovery of mesons.* * The discovery of mesons, unlike that of positive electrons, was not the result of a single observation, but rather the conclusion of a long series of experimental and theoretical investigations.

In 1932 Rossi (RB32.1), using the coincidence method invented by Bothe and Kolhörster (BW29), had shown that the cosmic radiation observed at seal level consists, in part, of particles capable of penetrating as much as one meter of lead. Shortly afterwards he also called attention to the existence of two different components of cosmic rays. The particles of the first component (penetrating component) could traverse large thicknesses of matter and were absorbed by different substances in approximate proportion to their mass. The particles of the second component (shower-producing component) were readily absorbed, especially by heavy elements, and their absorption was accompanied by abundant production of secondary rays (showers) (RB33.1; RB33.2; RB34). Cloud chamber experiments of Anderson and Neddermeyer (ACD34) on the passage of cosmic rays through lead plates also suggested the existence of two different types of cosmic-ray particles. These experiments showed that, whereas the *average* energy loss of cosmic-ray particles in lead was of the order of magnitude of the computed collision loss (§ 2.5), some of these particles suffered considerably larger losses.

In 1934 Bethe and Heitler (BHA34) published the theory of radiation losses by electrons and pair production by photons (§§ 2.11 and 2.19). The properties of the more "absorbable" particles observed by Anderson and Neddermeyer were found to be in agreement with the properties of electrons predicted by the theory of Bethe and Heitler, the large energy losses being explained by radiation processes. Also, the properties of the shower-producing radiation observed by Rossi could be explained under the assumption that this radiation consists of high-energy electrons and photons (see Chapter 5). On the other hand, if one granted the validity of Bethe and Heitler's theory one was forced to the conclusion that the "penetrating" particles in Rossi's experiments and the less "absorbable" particles in Anderson and Neddermeyer's experiments were different from electrons. Indeed, since the theoretical energy loss by radiation is inversely proportional to the square of the mass, it was necessary to assume that the penetrating particles were heavier than electrons.

The possibility of a breakdown of the radiation theory at high energies was seriously taken into consideration. As an alternative, Williams in 1934 suggested that the penetrating particles in cosmic rays might be of protonic mass (WEJ34). A difficulty of this assumption was that it required the existence of *negative* as well as positive protons, because cloud-

* On this subject, see also ref. (NSH39).

chamber experiments had shown that penetrating particles in cosmic rays have charges of both signs. Moreover, in some of the cloud-chamber pictures taken by Anderson and Neddermeyer (ACD34) one could see particles that did not radiate like electrons and yet did not seem to be as massive as protons. Thus by the end of 1936 it appeared very likely that cosmic rays contained, in addition to electrons, particles of a hitherto unknown type, presumably particles with mass intermediate between those of the electron and the proton. One may also add that in 1935 Yukawa, on purely theoretical grounds, had predicted the existence of such particles.

Direct experimental proof for the existence of particles with intermediate mass came in 1937 from the observations of Neddermeyer and Anderson and those of Street and Stevenson.

The experiments of Neddermeyer and Anderson (NSH37) were a continuation, with improved technique, of the work on the energy loss of cosmic-ray particles mentioned above (ACD34; ACD36). They were performed by means of a cloud chamber separated into two halves by a

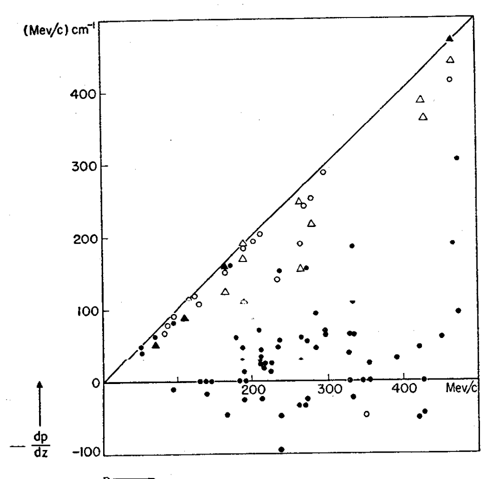

Fig. 4.6.1. Momentum loss per centimeter of platinum of cosmic-ray particles, $-dp/dz$, plotted as a function of incident momentum, p. ●: single particles traversing the absorber without producing secondary effects. ▲: single particles producing showers in the absorber. ○: particles occurring in groups and traversing the absorber without producing secondary effects. △: particles occurring in groups and producing showers in the absorber. From Neddermeyer and Anderson (NSH37).

1-cm-thick platinum plate and operated in a magnetic field. The momentum losses of individual cosmic-ray particles were determined by measurement of the track curvature above and below the plate (§ 3.13). In Fig. 1 each point represents the result of a separate measurement. The abscissa is the momentum of the incident particle in Mev/c and the ordinate is its momentum loss in Mev/c per centimeter of platinum. One will notice that the points fall rather distinctly into two groups: an "absorbable" group for which the momentum losses are comparatively large and increase in proportion to the initial momentum, and a "penetrating" group for which the momentum losses are comparatively small and do not depend strongly on momentum.

The absorbable particles can easily be interpreted as electrons. This interpretation is strengthened by the observation that the absorbable particles, unlike the penetrating particles, often give rise to secondary effects in the platinum absorber and mostly occur in groups of two or more. This is what one should expect, because many of the electrons observed with an arrangement of the type used by Neddermeyer and Anderson are part of showers produced in the neighboring materials. With regard to the nature of the penetrating particles, the two most illuminating results obtained by Neddermeyer and Anderson are the following:

(1) Even though absorbable particles are relatively more abundant at low momenta and penetrating particles are relatively more abundant at high momenta, *there exists a momentum interval in which both absorbable and penetrating particles are present.* Thus the difference in behavior of the two kinds of particles cannot be accounted for by a difference in energy. This result rules out the possibility of identifying penetrating particles with electrons and explaining their behavior by a breakdown of the radiation theory at high energies.

(2) *There exist a number of penetrating particles with momenta smaller than 200 Mev/c that do not ionize more heavily than a singly charged particle near the minimum of the ionization curve.* This means that the penetrating particles in cosmic rays are considerably lighter than protons, as a proton of less than 200 Mev/c momentum has a specific ionization about ten times minimum.

Street and Stevenson (SJC37) attempted to estimate the mass of cosmic-ray particles directly by simultaneous measurements of momentum and specific ionization. They used a cloud chamber triggered by an anticoincidence arrangement of Geiger-Mueller counters designed to select particles near the end of their range. The chamber was operated in a magnetic field of 3500 gauss and the expansions were delayed about one second to permit drop-counting (§ 3.12). Among a large number of pictures, Street and Stevenson found one of exceptional interest, which is reproduced in Fig. 2. This picture shows the track of a particle of

29 Mev/c momentum with about 6 times minimum ionization. If the particle travels in the downward direction, its sign is negative. *From the momentum and the specific ionization, its mass turns out to be approximately 175 electron masses* with a probable error of 25 per cent due to uncertainty in the measurement of the specific ionization.* Note that

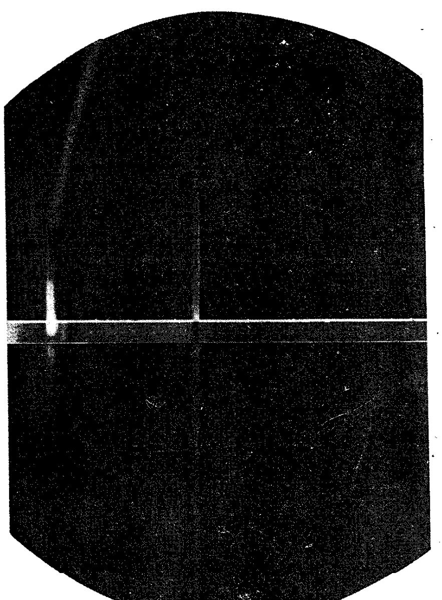

Fig. 4.6.2. Cloud-chamber picture of a meson. From Street and Stevenson (SJC37).

an electron of 29 Mev/c has practically minimum ionization. On the other hand, a particle with this momentum and with protonic mass (either a normal proton traveling upward or a *negative* proton traveling downward) has a specific ionization about 200 times minimum and a range in the gas of the chamber of less than one centimeter. The track in question instead was clearly visible for 7 cm, after which it passed out of the illuminated region.

* The value quoted in the original paper (130 electron masses) had been computed on the basis of an inaccurate relation between specific ionization and velocity.

The experiments described above proved beyond any doubt that the penetrating particles in cosmic rays are actually heavier than electrons and lighter than protons. Moreover the experiment of Street and Stevenson provided the first approximate evaluation for the mass of this new particle, which we may now call by its accepted name of *meson*.*

4.7. *The instability of mesons. Determination of the mean life.* Early experiments on the variation of intensity of cosmic-ray particles with altitude and with zenith angle had shown certain anomalies that were difficult to explain in terms of energy loss in the atmosphere (FDH36; AP37; EA37). Cosmic-ray particles appeared to undergo a stronger absorption in air than in condensed materials, when layers of the same mass per unit area were compared. Also, the decrease of cosmic-ray intensity with increasing zenith angle appeared to be steeper than one would have anticipated by simply considering the greater mass of atmosphere traversed by particles coming from inclined directions.

In 1938 Kulenkampff (KIH38) pointed out that one could explain these anomalies by assuming that mesons are unstable (as suggested by Yukawa's theory; § 4.18) and have a mean life comparable with their time of flight in the atmosphere. Indeed, if this is the case, some of the mesons traveling in the atmosphere will disappear by spontaneous decay before reaching the end of their range. In condensed absorbers, instead, decay will play a negligible role because of the much shorter distance in which mesons are brought to rest by ordinary energy losses. Therefore the apparent absorption per g cm^{-2} will be greater in air than in condensed absorbers. Moreover the absorption in air will increase with decreasing density. The latter effect explains the fact that the intensity is greater at the depth x in the vertical direction than it is at the depth $x \cos \theta$ in a direction forming and angle θ with the vertical. In both cases the thickness (in g cm^{-2}) of the atmosphere in the direction of observation is the same. But the average density of air is greater along the vertical path at the depth x than along the inclined path at the depth $x \cos \theta$.

In the subsequent years Rossi and his collaborators (RB40.1; RB41.2; RB42.1) as well as other experimenters (NWM40, NWM41; NHV40; PMA40; AM40; DGN40; BG41) made a systematic investigation of the absorption anomalies. Their measurements confirmed the disintegration hypothesis and provided a first quantitative estimate of the mean life of mesons. Rossi, Hilberry, and Hoag (RB40.1) for example, used a cosmic-ray telescope, selecting particles (for the most part mesons) incident in nearly vertical directions and capable of traversing 12.7 cm of lead. They took measurements near sea level and at various altitudes in the mountains, both with and without a layer of 87 g cm^{-2} of carbon above the instrument. Their results are shown in Fig. 1, where the abscissa represents

* Earlier names, now outmoded: *barytron*, *yukon*, *mesotron* (the last, however, is still used by some authors).

the total thickness of matter (air plus carbon) above the instrument and the ordinate is the logarithm of the corresponding counting rate recorded by the cosmic-ray telescope. The solid curve connecting experimental points obtained without carbon represents essentially the variation of the vertical meson intensity with depth below the top of the atmosphere. The dashed lines connecting pairs of points obtained at any one location with and without carbon absorbers give the initial slopes of the logarithmic absorption curves of mesons in carbon. One sees that these slopes are

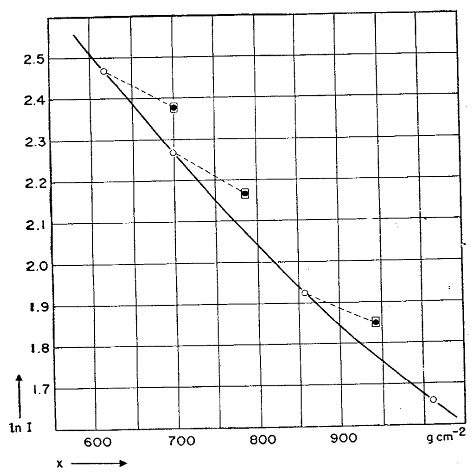

Fig. 4.7.1. Comparison between the absorption of cosmic-ray mesons in air and carbon. The solid line represents the logarithm of the intensity of mesons, ln I (in arbitrary units), as a function of atmospheric depth, x. The dashed lines represent the result of absorption measurements in carbon. From Rossi *et al.* (RP 40.1).

only about one-half as large as the corresponding slopes of the absorption curve in air. Since collision losses in air and carbon are approximately the same (§ 2.6), this result indicates that the absorption of mesons in air is due in approximately equal parts to decay and to normal energy losses. The above measurements, along with a reasonable assumption for the momentum distribution of mesons, gave a value of $2.5 \cdot 10^{-8}$ microseconds/ev for the ratio τ/mc^2 of the mean life to the rest energy of mesons. With the presently accepted value of the rest energy ($mc^2 = 1.07 \cdot 10^8$ ev; § 4.13) the corresponding mean life is $\tau = 2.7$ microseconds.

The following is a more rigorous discussion of the decay of mesons in flight. Consider a meson traveling vertically downward through the atmosphere. Let m be its mass and $p(x)$ its momentum at the atmospheric depth x. Assume that the meson is observed at the depth x_1. We ask for the probability, $w(x_1,x_2)$, that this meson does not decay before reaching the atmospheric depth x_2.

If τ is the mean life of the meson at rest, the apparent mean life of a meson moving with a velocity βc is $\tau/\sqrt{1-\beta^2}$. The average distance traversed by the meson before it disintegrates is thus;

$$z_d = \frac{\beta c\tau}{\sqrt{1-\beta^2}} = \frac{p\tau}{m}, \tag{1}$$

and the probability for the meson to disintegrate while traversing an infinitesimal layer of thickness dx has the expression:

$$\frac{dx}{\rho z_d} = \frac{z_0 m}{\tau p}\frac{dx}{x},$$

where ρ is the density of air at the depth x and $z_0 = x/\rho$. One thus obtains for w the following differential equation:

$$-dw = w\frac{z_0 m}{\tau p}\frac{dx}{x}. \tag{2}$$

Integration of Eq. (2) with the boundary condition $w(x_1,x_1) = 1$ (expressing the assumption that the meson has not decayed before reaching the depth x_1) yields:

$$-\ln w(x_1,x_2) = \int_{x_1}^{x_2} \frac{z_0}{\tau}\frac{m}{p(x)}\frac{dx}{x}. \tag{3}$$

Because of the collision loss, the momentum p of the meson is a decreasing function of x. The quantity z_0 is a constant in an isothermal atmosphere. In the real atmosphere z_0 is a slowly varying function of x (see Appendix 6). If the depth interval from x_1 to x_2 is not too large we may consider z_0 as independent of x. If, moreover, the meson is not too close to the end of its range when it reaches the depth x_2 we may assume the momentum loss to be independent of x and use for p the expression:

$$p(x) = p(x_1) - a(x - x_1),$$

where a is a constant. Eq. (3) then becomes:

$$-\ln w(x_1,x_2) = \frac{z_0 m}{\tau}\int_{x_1}^{x_2}\frac{dx}{[p(x_1) - a(x - x_1)]x},$$

from which one obtains:

$$-\ln w(x_1,x_2) = \frac{z_0 m}{\tau}\frac{1}{p(x_1) + ax_1}\ln\left[\frac{x_2\,p(x_1)}{x_1\,p(x_2)}\right]. \tag{4}$$

One will notice that the survival probability, w, depends on the ratio τ/m. Thus from measurements on the decay of mesons in flight one cannot determine the value of the mean life of mesons directly, but the ratio of the mean life to the mass (or the rest energy) of the mesons.

Final proof of the meson decay hypothesis came from direct observation of the decay products in cloud-chamber pictures and by means of delayed-coincidence experiments.

The first cloud-chamber picture of meson decay was obtained by Williams and Roberts in 1940 (WEJ40.1). This picture shows a track identifiable as that of a meson coming to rest in the gas of the chamber and the track of what appears to be a positive electron coming out of the end of the meson track.* A clear example of a similar event, photographed several years later by Thompson (TRW48) is reproduced in Fig. 2. This cloud-chamber picture, taken in a magnetic field of 1680 gauss, shows the track of a positive particle with minimum or nearly minimum ionization that becomes very heavily ionizing after traversing a 0.63-cm aluminum

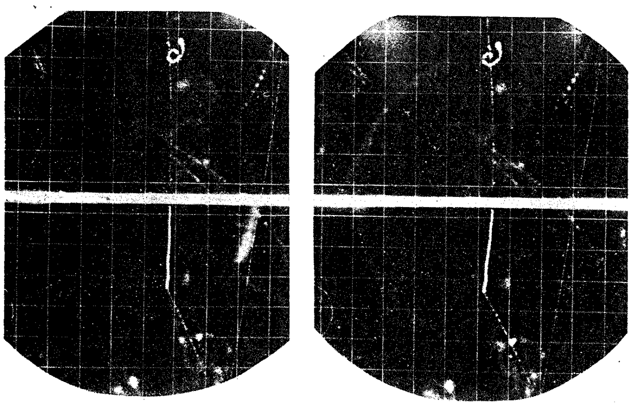

Fig. 4.7.2. Stereoscopic photographs of a meson stopping in the gas of a cloud chamber and disintegrating with the emission of an electron. From R. W. Thompson (TRW48).

plate, in which it apparently loses most of its energy. The particle then comes to rest in the gas of the chamber and the track of a positive particle with minimum ionization is seen to originate from the point where the track of the first particle ends. The momentum of the incident particle above the aluminum plate cannot be measured with sufficient accuracy to afford a precise mass determination. It is certain, however, that the incident particle is a meson, because a proton with range approximately equal to 0.63 cm aluminum would have a specific ionization about 5 times minimum and would not exhibit any appreciable curvature in a magnetic field of 1680 gauss. Similarly, from the curvature and the specific ionization of the secondary particle one can conclude that this particle is considerably lighter than a meson, and it is thus almost certainly an electron.

* For other early pictures of meson decay, see (WEJ40.2; JTH42; SRP42).

The delayed emission of charged particles from absorbers in which mesons have come to rest was first observed by Rasetti in 1941 (RF41). Rasetti's experimental arrangement is shown schematically in Fig. 3. Circles represent Geiger-Mueller counters; counters designated by the same letter are connected in parallel. With the lead absorbers placed in the positions shown by the diagram, coincidences between counters A, B, C, and D are mostly due to mesons. Some of these mesons stop in a block or iron or aluminum marked "absorber" and thus fail to discharge counters F. When this happens, an anti-coincidence $(ABCD - F)$ occurs. Suppose that the mesons, after coming to rest in the absorber, disintegrate

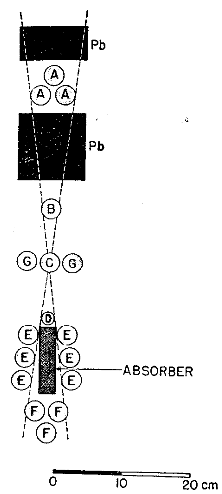

Fig. 4.7.3. Experimental arrangement used by Rasetti to demonstrate the decay of mesons (RF41). (Explanation in the text. The black area represents lead; the two counters, G, are connected in anti-coincidence and serve to decrease the effect of side showers).

with a finite mean life and give rise to secondary electrons, as shown by the cloud-chamber pictures. The decay electrons have a certain probability of discharging one of the lateral counters, E. Consequently some of anti-coincidence $(ABCD - F)$ will be followed, with small delays, by discharges of counters E. Rasetti succeeded in demonstrating the existence of this effect by recording coincidences between events $(ABCD - F)$ and pulses of counters E simultaneously with three circuits of different resolving times, approximately 1, 2, and 15 microseconds respectively. He found that the 1-microsecond channel recorded fewer coincidences than the 2-microsecond channel, and this channel recorded fewer coincidences than the 15-microsecond channel. In other words, there were pulses of counters E following $(ABCD - F)$ events with delays from 1 to 2 microseconds and from 2 to 15 microseconds. From the ratios of the coincidence rates in the three channels (corrected for chance coincidences) Rasetti obtained an estimate of 1.5 microseconds for the mean life of mesons in the absorber.

Rossi and Nereson (RB42.3; NNG43) as well as other experimenters (CR44; CM44; THK48.1; THK48.2) investigated the delayed emission of electrons with improved experimental techniques and thus succeeded in determining the mean life of mesons accurately. The arrangement of absorbers and counters used by Rossi and Nereson was similar to that used by Rasetti (Fig. 3). The pulses of the counters recording the arrival of mesons upon the absorber, and those of the counters detecting the emission of decay electrons from the absorber, were fed to the two separate inputs of a time-measuring circuit. This circuit gave an output pulse whose amplitude was a function of the time separation between the two input pulses. A pen-writing instrument registered the output pulses of the time-measuring circuit and thus recorded the time of survival in the absorber of all mesons whose decay electrons discharged one of the lateral counters.

Rossi and Nereson experimented with absorbers of lead, brass, and aluminum. For reasons that will become clear later (§ 4.9) we consider here only the results obtained with brass and lead. These are shown in Fig. 4, where the abscissa represents the time interval, t, between the arrival of a meson upon the absorber and the emission from the absorber of the corresponding decay electron, and the ordinate represents, on a logarithmic scale, the total number of events for which t is greater than the corresponding abscissa. The curves drawn through the experimental points have exactly the same meaning as the disintegration curves of radioactive substances. Indeed, they give the number of mesons whose life span in the absorber is greater than a certain time interval t. One sees that, within the experimental errors, the disintegration curves of mesons in brass and lead are represented by straight parallel lines on the semilogarithmic plot, which means that mesons decay exponentially, much as radioactive atoms do, and that the mean life of mesons in the two absorbers is the same. Analysis of the experimental data by the method of least squares gave the following value for the mean life of mesons:

$$\tau = 2.15 \pm 0.1 \text{ microseconds}, \qquad (5)$$

where the error corresponds to statistical inaccuracy.

The variable spontaneous time-lags of Geiger-Mueller counters (§ 3.6) make it impossible to follow the disintegration curve of mesons much below 1 microsecond. On the other hand, one can show that these time-lags do not affect the shape of the disintegration curve for values of t greater than t_1, where t_1 represents the maximum value of the spontaneous

Fig. 4.7.4. Integral disintegration curves of mesons in lead and brass. Each point represents the observed number, N, of decay events for which the delay is greater than t. From N. Nereson and B. Rossi (NNG43).

time-lags.* Thus the existence of spontaneous time-lags in Geiger-Mueller counters does not introduce any error in the determination of the mean life of mesons if delays smaller than t_1 are disregarded.

Values of τ in substantial agreement with that obtained by Rossi and Nereson were reported by Chaminade, Freon, and Maze (CR44), by Conversi and Piccioni (CM44), and by Ticho and Schein (THK48.1; THK48.2).

Several years later the artificial production of mesons (see § 4.10) made it possible to determine the mean life of these particles with greater precision than one can obtain from cosmic ray experiments. Preliminary

* The reason for this is, essentially, that if a function, $f(t)$, is proportional to $\exp(-t/\tau)$, the function $f(t + t_0)$ with t_0 constant is also proportional to $\exp(-t/\tau)$ (RB42.3). For a more detailed discussion of the effect of spontaneous delays, see also (BD49).

measurements with artificially produced mesons by Alvarez and his collaborators (ALW50) gave the result:

$$\tau = 2.09 \pm 0.03 \text{ microseconds.} \tag{6}$$

4.8. ***The π-meson and the μ-meson.*** In 1947 Lattes, Occhialini, and Powell (LCM47.1), working with the newly developed Ilford Nuclear Research emulsions (§ 3.14), observed several events of the type represented in Fig. 1. In this picture one sees the track of a particle (marked π) entering the emulsion from the outside and coming to rest in the emulsion.

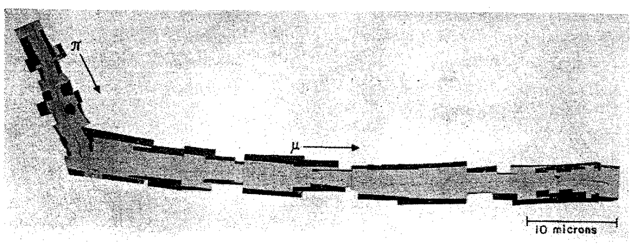

Fig. 4.8.1. Mosaic of microphotographs showing a $\pi \to \mu$ decay in Ilford C2 emulsion. From Lattes *et al.* (LCM47.1).

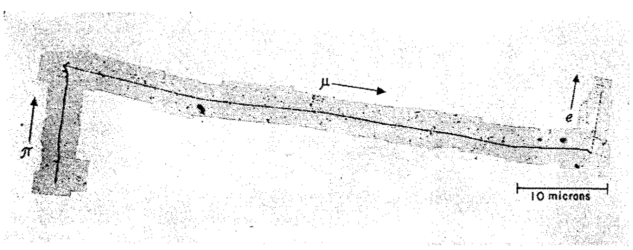

Fig. 4.8.2. Mosaic of microphotographs showing a $\pi \to \mu \to e$ decay. Kodak NT4 electron sensitive emulsion. From Brown *et al.* (BRH49.2).

The direction of the motion is indicated unambiguously by the gradual increase in grain density, which accompanies the decrease in velocity of the particle. Comparison with proton tracks recorded in the same emulsion shows that the particle in question is a meson. From the point where this meson comes to rest the track of another particle originates, marked μ. This track also ends in the emulsion and again can be identified as that of a meson. However, accurate measurement of grain density as a function of range (§ 3.16) shows that the particle marked μ is somewhat lighter than the particle marked π.

Lattes, Occhialini, and Powell interpreted their observations as proof for the existence of two different kinds of mesons with somewhat different masses, of which the lighter arises from the heavier through a spontaneous decay process. They called the primary (heavier) meson *π-meson*, the secondary (lighter) meson, *μ-meson*.

The meson with 2.1-microsecond lifetime, which, according to the experimental results described in § 4.7, is the main constituent of the penetrating component of cosmic rays, cannot possibly be identified with the π-meson, because when it disintegrates it gives rise to an electron and not to a secondary meson. Lattes, Occhialini, and Powell tentatively identified the 2.1-microsecond meson with the μ-meson. If this is correct, μ-mesons, after coming to rest in the emulsion, should give rise to electrons by spontaneous decay. The emulsions used by Lattes and his collaborators were not sensitive to particles with minimum ionization and, therefore, could not record the decay electrons, if any were produced. Later, however, Brown, Camerini, Fowler, Muirhead, Powell and Ritson (BRH49.2), working with electron-sensitive emulsions, succeeded in detecting the expected disintegration of μ-mesons and thus confirmed the assumption concerning the nature of these particles. An example of the events recorded by Brown and her collaborators is reproduced in Fig. 2. This picture clearly shows a π-meson that comes to rest in the emulsion and gives rise to a μ-meson, which, in turn, comes to rest in the emulsion and gives rise to a particle with minimum ionization, presumably the decay electron.

The above results naturally suggest the hypothesis that the μ-mesons present in cosmic rays arise entirely from the decay of π-mesons. If this is the case, from the large ratio between the numbers of μ-mesons and π-mesons in the atmosphere one must necessarily conclude that the mean life of π-mesons is much shorter than that of μ-mesons. Direct measurements, to be discussed in § 4.14, confirm this conclusion.

4.9. ***Nuclear absorption of μ-mesons and π-mesons.*** In 1940 Tomonaga and Araki (TS40) pointed out that positive and negative mesons should behave differently after coming to rest in matter. A positive meson (whether π or μ) slowed down to thermal velocity by inelastic collisions is repelled by atomic nuclei. Therefore it can never approach a nucleus at a sufficiently close distance for an interaction to occur, and it eventually disappears by spontaneous decay. A negative meson, however, is promptly captured into a Bohr orbit in the neighborhood of a nucleus and has, therefore, a chance of being absorbed by the nucleus before it undergoes spontaneous decay.

Conversi, Pancini, and Piccioni (CM45; CM47) were the first to demonstrate experimentally the different behavior of positive and negative mesons at rest. They used cosmic rays as a source of mesons and consequently their observations refer to μ-mesons. The aforementioned authors, following a method originated by Rossi in 1931 (RB31), took advantage of the deflection of charged penetrating particles in magnetized iron to build a "magnetic lens;" i.e., a device that, depending on the direction of magnetization, concentrates either positive or negative slow mesons upon an absorber. The experimental arrangement is shown schematically in Fig. 1. A, B, and C represent Geiger-Mueller counters. F_1 and F_2 are two bars of iron, magnetized in the two opposite directions parallel to the axes

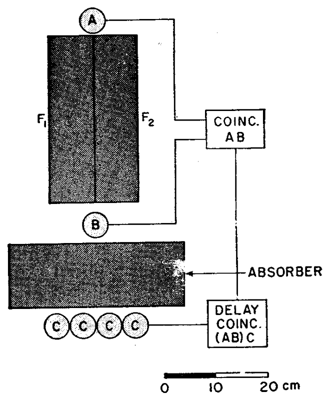

Fig. 4.9.1. Schematic diagram of the experimental arrangement used by Conversi *et al.* (CM45; CM47) to investigate the behavior of positive and negative mesons at the end of their range. F_1 and F_2 are two bars of iron magnetized in opposite directions. A, B, are Geiger-Mueller tubes selecting mesons. Below B there is an absorber where the mesons come to rest. C are Geiger-Mueller tubes detecting decay electrons.

of the Geiger-Mueller counters. Counters A and B are connected to a coincidence circuit. Counters C are connected in parallel. The pulses of counters C and the output pulses of the coincidence circuit (AB) go to a "delayed coincidence circuit." This circuit registers a coincidence whenever a pulse of the coincidence circuit (AB) is followed by a pulse of counters C with a delay longer than a predetermined minimum value, t_{min}, and shorter than a predetermined maximum value, t_{max} (in the experiments in question, $t_{min} = 1$ microsecond, $t_{max} = 4.5$ microseconds). Thus the experimental arrangement is capable of detecting μ-mesons that traverse counters A and B, come to rest in the absorber, and subsequently decay giving rise to electrons that discharge counters C. Suppose that the iron

bars are magnetized as shown in Fig. 2; i.e., with the magnetic induction vector $\mathfrak{B}$ pointing toward the observer in the bar to the right (F_2) and away from the observer in the bar to the left (F_1). One will see that the magnetic field deflects positive mesons in such a way as to *increase* the number of those traversing counters A and B (Fig. 2a), whereas it deflects negative mesons in such a way as to *decrease* the number of those traversing these counters (Fig. 2b). The opposite situation exists when the field is reversed.

Conversi, Pancini, and Piccioni designed their experimental arrangement so that it would reject almost all mesons of the wrong sign and with

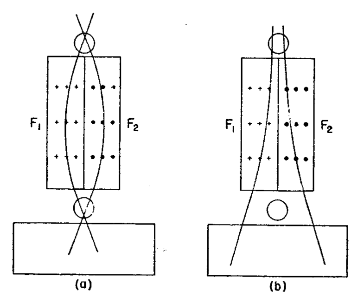

Fig. 4.9.2. Illustrating the operation of a magnetic lens.

sufficiently small energy to be stopped by the absorber.* In a first experiment (CM45), they showed that when μ-mesons are brought to rest in *iron*, only the positive ones undergo spontaneous decay. In a second experiment, however, (CM47), they showed that in a *carbon* absorber, both positive and negative μ-mesons undergo spontaneous decay. These results indicated that negative μ-mesons, after coming to rest in an absorber of high atomic number, mostly undergo nuclear absorption, whereas, after coming to rest in an absorber of low atomic number, they mostly undergo spontaneous decay.

The results described above were extended and made more precise by the work of Valley (VGE47; VGE49), Sigurgeirsson and Yamakawa (ST47), Ticho and Schein (THK48.1), Valley and Rossi (VGE48), and Ticho (THK48.2). Before discussing these experiments it may be appropriate to consider in more detail the expected observable results of a

* Note that in all media, including ferromagnetic media, the deflecting force on a moving charge is determined by the magnetic induction, $\mathfrak{B}$. For a quantitative discussion of the operation of magnetic lenses the reader may consult a paper by Bernardini and his collaborators (BC45).

competition between spontaneous decay and nuclear absorption of negative μ-mesons.

Theoretical considerations show that, in all elements, the time for capture of a negative meson into a Bohr orbit is a negligible fraction of the mean life of μ-mesons before decay (WJA47; FE47.1; FE47.2). Thus we may assume that a negative μ-meson coming "to rest" in an absorber becomes immediately part of an atom, replacing one of the atomic electrons. Its wave function has a certain finite density at the nucleus; therefore the meson may interact with nuclear particles, if it is at all capable of such interaction.

Let dt/τ_a represent the probability for an interaction leading to the disappearance of a negative μ-meson to occur in the time interval, dt; thus τ_a represents the mean life before nuclear absorption of negative μ-mesons. During the same time interval, the probability for the meson to undergo spontaneous decay is dt/τ, where τ is the natural mean life of μ-mesons. One sees immediately that the ratio between the number of mesons that undergo spontaneous decay and the number of mesons that undergo nuclear absorption is τ_a/τ, so that the fractional number of those that decay is:

$$f = \frac{\tau_a}{(\tau + \tau_a)}. \tag{1}$$

The total probability for the meson to disappear during the time interval, dt, either by spontaneous decay or by nuclear absorption, is:

$$\frac{dt}{\tau} + \frac{dt}{\tau_a} = dt\left(\frac{1}{\tau} + \frac{1}{\tau_a}\right).$$

It follows that the probability of survival of negative μ-mesons in an absorber where nuclear absorption occurs is still an exponential function of time: $\exp[-t/\tau^{(-)}]$. The apparent mean life, $\tau^{(-)}$, however, is shorter than the mean life τ for spontaneous decay and is given by the equation:

$$\frac{1}{\tau^{(-)}} = \frac{1}{\tau} + \frac{1}{\tau_a}. \tag{2}$$

By combining Eq. (1) with Eq. (2) one obtains the following relation between the apparent mean life of negative μ-mesons, $\tau^{(-)}$, and the fractional number, f, of negative μ-mesons that undergo spontaneous decay:

$$f = \frac{\tau^{(-)}}{\tau}. \tag{3}$$

These conclusions were submitted to test by various experimenters (THK48.1; THK48.2; VGE48; VGE49). To separate positive from negative mesons, Ticho and Schein used a magnetic lens similar to that used by Conversi and his collaborators; Valley and Rossi, instead, used a cloud chamber in a magnetic field.

The experimental arrangement of Valley and Rossi is shown in Fig. 3. CC represents a cloud chamber, which is operated in a magnetic field of about 6,000 gauss; 1, 2, and 3 are three trays of Geiger-Mueller counters forming a vertical cosmic-ray telescope; S is the absorber under investigation; D are Geiger-Mueller counters, which detect the electrons produced by the disintegration of mesons stopped in S. The cloud chamber is expanded whenever a coincidence (1,2,3) marking the arrival of a meson upon the absorbers is followed by a pulse in one of counters D after a time longer than 1 and shorter than 9 microseconds. The actual time interval between the arrival of the meson and the emission of the electron is recorded by an electronic device whose output operates a ballistic galvanometer. The galvanometer dial is photographed

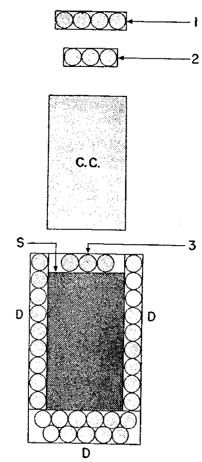

Fig. 4.9.3. Experimental arrangement used by Valley to measure the disintegration curves of positive and negative mesons. The Geiger-Mueller trays, 1,2,3, form a telescope selecting nearly vertical mesons. S is the absorber in which the mesons come to rest. The Geiger-Mueller counters, D, surrounding the absorber, S, detect electrons produced by decaying mesons. $C.C.$ is the cloud chamber operating in a magnetic field of about 6,000 gauss.

simultaneously with the cloud chamber. Thus from each individual picture one obtains information on the sign and on the momentum of the meson that has come to rest in the absorber as well as on its time of survival. The measurement of the momentum together with the knowledge of the absorber thickness enables one to set limits to the mass of the particles absorbed and thus to check that these particles are actually μ-mesons.

Ticho and Schein as well as Valley and Rossi measured the disintegration curves of positive and negative mesons separately in substances of different atomic numbers. They found that each disintegration curve follows an exponential law, within the accuracy of the experiments. The disintegration curves of positive mesons in all substances were consistent with a mean life of 2.1 microseconds. The disintegration curves of negative μ-mesons showed that the mean life of these particles decreases gradually as the atomic number Z increases. It is practically identical to the mean life of positive μ-mesons around $Z = 4$ and becomes small compared with 1 microsecond around $Z = 20$.

Figure 4 shows, as an example, a set of disintegration curves for positive and negative μ-mesons, obtained by Valley in aluminum. Under the assumption that nuclear capture of negative μ-mesons does not give rise to particles capable of discharging Geiger-Mueller counters (§ 4.12) extrapolation to $t = 0$ of the disintegration curves in Fig. 4 (and of similar curves measured in other substances) gives the relative numbers of negative and positive mesons that have undergone spontaneous decay during the time of observation. From these numbers, and from the ratio of negative to positive μ-mesons near sea level* one can compute the fractional number, f, of negative μ-mesons that undergo spontaneous decay in the various substances.

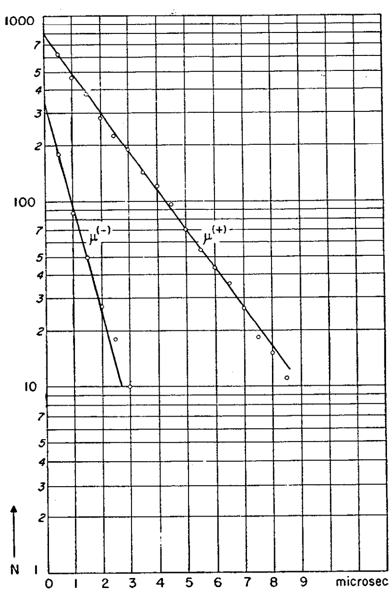

Fig. 4.9.4. Disintegration curves of positive and negative μ-mesons in aluminum; measured by Valley with the experimental arrangement shown in Fig. 4.9.3. The straight lines correspond to mean lives of 2.06 and 0.81 microseconds, respectively. (Private communication.)

* This ratio is probably somewhat less than 1, but its value is not known accurately. Also, it may depend on the meson energy. Thus one cannot evaluate f with great precision. Other sources of errors that should be considered and corrected for are mentioned in ref. (VGE48).

The experimental results obtained by Ticho and by Valley are summarized in Table 1. The approximate equality between the values of $\tau^{(-)}/\tau$ and the corresponding values of f confirms the assumption that the shortening of the mean life of negative μ-mesons is actually due to competition between nuclear absorption and spontaneous decay.*

Table 4.9.1. Mean lives, $\tau^{(-)}$, of negative μ-mesons and fractional numbers, f, of negative μ-mesons that undergo spontaneous decay in various substances.

Substance	Z	$\tau^{(-)}$ (microseconds)	τ^-/τ^+	f	Author
H_2O*	8	1.89 ± 0.15	0.877 ± 0.069	0.833 ± 0.083§	H. K. Ticho (THK48.2)
NaF†	10.1	1.28 ± 0.12	0.595 ± 0.060	0.602 ± 0.060§	H. K. Ticho (THK48.2)
Mg	12	0.96 ± 0.06	0.446 ± 0.032	0.558 ± 0.044§	H. K. Ticho (THK48.2)
Al	13	0.75 ± 0.07	0.34 ± 0.03	0.40 ± 0.03§	H. K. Ticho (THK48.2)
Al	13	0.81 ± 0.06	0.40 ± 0.03	0.43 ± 0.04¶	G. E. Valley‡
S	16	0.54 ± 0.12	0.25 ± 0.04	0.28 ± 0.03§	H. K. Ticho (THK48.2)

* Only oxygen is effective; when the meson stops in the vicinity of a hydrogen nucleus the two particles form a neutral system. Within the lifetime of the μ-meson, this system makes several thousand collisions with oxygen nuclei, in which the meson may attach itself to the oxygen (THK48.2).

† Computed under the assumption that the probability for a meson to stop in the neighborhood of any atom in a compound is proportional to the atomic number of this atom (FE47.2).

‡ Private communication.

§ Computed under the assumption that the number of positive mesons is 20 per cent greater than that of negative mesons.

¶ Computed under the assumption that the numbers of positive and negative mesons are equal.

The dependence on atomic number of the mean life before nuclear absorption, which manifests itself in the rapid change of $\tau^{(-)}$ with Z, has a simple theoretical explanation (WJA47). The probability of nuclear absorption for a meson that has been captured into a Bohr orbit is proportional to the number of protons in the nucleus and to the probability for the meson to be in the nucleus. The number of protons is equal to the atomic number. As the atomic number increases, the dimensions of the Bohr orbit decrease and therefore the amplitude of the meson wave function at the nucleus increases. On both accounts, the probability of nuclear absorption is an increasing function of the atomic number.

* Further experimental results on the capture probability of μ^--mesons in heavy elements are described in ref. (HFB51).

For light elements, the radius of the nucleus is small compared with the Bohr radius of the meson orbit.* Therefore the nucleus may be considered as a point charge. In this case the Bohr radius is inversely proportional to Z, which makes the amplitude squared of the meson wave function at the nucleus proportional to Z^3. Therefore the probability of nuclear absorption is proportional to $Z^3 \cdot Z = Z^4$.

For heavy elements one should expect important deviations from the Z^4-law because the dimensions of the nucleus are not small compared with those of the Bohr orbit, so that the meson is, for a considerable fraction of the time, inside the nucleus. Wheeler (WJA49) has computed the dependence of the capture probability on atomic number, taking into account the finite dimensions of the nucleus. The results of the computation contain a constant, Z_0, which depends on the strength of the interaction between μ-mesons and nucleons and whose value may be found by comparison with the experimental data. The values of $\tau^{(-)}$ computed by Wheeler with $Z_0 = 7$ and $Z_0 = 10$ are listed in Table 2, along with the

Table 4.9.2. Theoretical and experimental values of the mean life of negative μ-mesons in various substances. [From Table 4.9.1 and from the computations of Wheeler (WJA49).]

Element	Z	$\tau^{(-)}(Z_0 = 10)$ (microseconds)	$\tau^{(-)}(Z_0 = 7)$ (microseconds)	$\tau^{(-)}$ Experimental (microseconds)
Be	4	2.10	1.96	
B	5	2.04	1.75	
C	6	1.93	1.47	
N	7	1.80	1.18	
O	8	1.62	0.91	1.89
F	9	1.43	0.70	
Na	11	1.07	0.41	
Mg	12	0.91	0.32	0.96
Al	13	0.77	0.25	0.75-0.81
S	16	0.48	0.137	0.54
Fe	26	0.142	0.036	
Zn	30	0.103	0.026	
Br	35	0.074	0.018	
Ag	47	0.043	0.011	
I	53	0.036	0.0088	
Ba	56	0.033	0.0081	
W	74	0.024	0.0058	
Pb	82	0.022	0.0052	
U	92	0.020	0.0048	
Large		0.013	0.0027	

* Note that the radius of a meson orbit is smaller than that of the corresponding electron orbit in inverse proportion of the masses of the two particles.

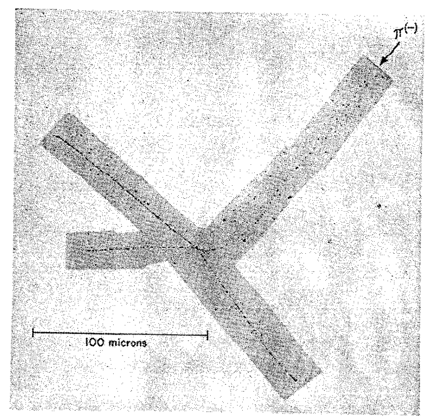

(a)

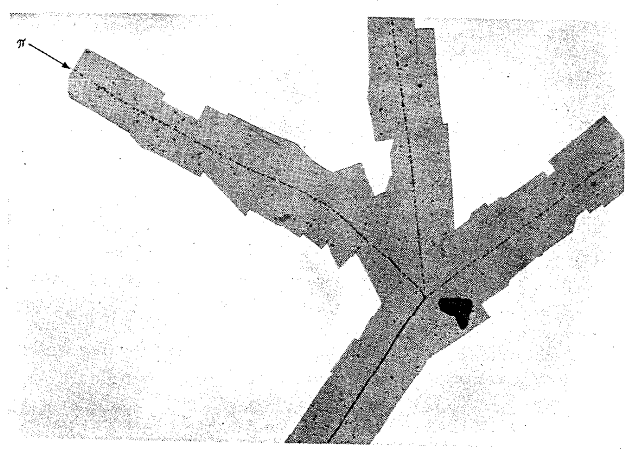

(b)

Fig. 4.9.5. Disintegrations produced by the nuclear absorption of negative π-mesons. (a) D. H. Perkins, Ilford B1 emulsion (PDH47). (b) Powell, Ilford C2 emulsion (PCF49).

experimental values of $\tau^{(-)}$, taken from Table 1. The experimental data favor the choice $Z_0 = 10$. With this choice of the constants the agreement between theoretical and experimental results is satisfactory.

The results discussed above show that if one wishes to determine the mean life of μ-mesons against decay without selecting positive mesons magnetically, one should use as an absorber either an element sufficiently heavy that practically only the decay of positive mesons is observed, or an element sufficiently light that the nuclear absorption of negative mesons is negligible. For elements of intermediate atomic numbers, the disintegration curve of μ-mesons is the sum of two exponentials, corresponding to the mean lives τ and $\tau^{(-)}$. If the measurements are not very accurate, and if $\tau^{(-)}$ is not very different from τ, the resulting curve may simulate a simple exponential and yield an apparent mean life intermediate between τ and $\tau^{(-)}$. For this reason, in § 4.7 we have disregarded the disintegration curve obtained by Rossi and Nereson in aluminum, even though this curve shows only a minor deviation from the natural disintegration curve of μ-mesons and yields practically the correct value of the mean life.

We have discussed so far the nuclear absorption of negative μ-mesons. The first experimental evidence for the nuclear absorption of negative π-mesons came from observations of cosmic-ray events in photographic emulsions. In 1947 Perkins (PDH47.1) and Occhialini and Powell (OGP47.2) obtained several pictures of the type shown in Figs. 5a and 5b. In both pictures one sees the track of a particle that, by the grain density and the scattering, can be identified as a slow meson. The change in grain density along the track determines the direction of the motion. The large density at the end of the track indicates that the particle has slowed down to a very small velocity and has presumably come to rest in the emulsion. At the place where the meson track ends there appears a "star"; i.e., a group of divergent tracks that may be identified as those of protons or other charged nuclear fragments. The star was interpreted as a nuclear explosion subsequent to the absorption of the meson at rest (presumably a negative meson) by a nucleus of one of the elements in the emulsion.

Further experiments by Lattes, Occhialini, and Powell (LCM47.4) showed that the number of mesons giving rise to nuclear disintegrations at the end of their tracks was of the same order of magnitude as the number of those giving rise to the $\pi \rightarrow \mu$ decay process described in § 4.8. This observation made it appear likely that mesons ending in stars were negative π-mesons rather than negative μ-mesons. Observations on artificially produced mesons, to be described in § 4.10, fully confirmed this interpretation.

In § 4.12 we shall return to the question of the nuclear absorption of negative mesons and discuss the reason why negative μ-mesons, when absorbed by nuclei, do not give rise to stars similar to those produced by negative π-mesons.

4.10. ***Experiments on artificially produced mesons.*** Experiments by means of artificially produced mesons have greatly added to our knowledge of the properties of these particles. Artificial production of mesons was first obtained at Berkeley in 1948 (GE48) by bombardment of various elements (beryllium, carbon, copper, uranium) with 380-Mev α-particles from the 184-inch cyclotron. Shortly afterwards, mesons were produced by means of high-energy protons, neutrons, and γ-rays (SFM50.1; GE50; MME49.1; MME49.2).

In the experiments on meson production by α-particle bombardment, the target in which mesons were produced, as well as the photographic plates used for their detection, were placed inside the vacuum chamber containing the circulating beam of α-particles. Positive and negative mesons emitted from the target were deflected in opposite directions by

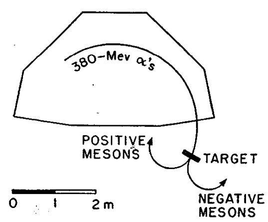

Fig. 4.10.1. Production of mesons in the internal α-particle beam of the Berkeley cyclotron. From J. Burfening *et al.* (BJ49).

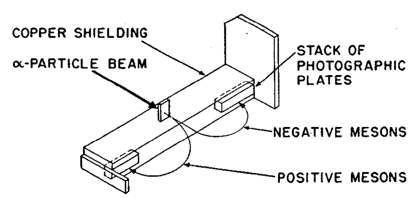

Fig. 4.10.2. Schematic diagram of an apparatus used for placing photographic plates below the circulating beam for exposure to both positive and negative mesons. From J. Burfening *et al.* (BJ49).

the magnetic field of the cyclotron (see Fig. 1). In the first experiments, only negative mesons were detected. In later experiments the photographic plates were so arranged as to detect both negative and positive mesons. Figures 2 and 3 show the details of two target-and-detector assemblies used in these experiments (BJ49).

In the apparatus shown in Fig. 2, the plates to receive positive and negative mesons are placed symmetrically on opposite sides of the target, slightly below the plane of the α-particle beam and parallel to this plane. Thus the apparatus detects mesons that leave the target at a small angle downward from the direction of the beam.

The apparatus shown in Fig. 3 makes use of only one stack of photographic plates, placed in the plane of the α-particle beam, outside of the circle covered by it. The plates receive negative mesons leaving the target in the forward direction on one edge, and positive mesons leaving the target in the backward direction on the other edge.

Fig. 4.10.3. Schematic diagram of an apparatus used for placing photographic plates in a position to receive negative mesons that leave the target in the direction of the beam, and positive mesons that leave the target in a direction opposite to the direction of the beam. From J. Burfening *et al.* (BJ49).

The first observations on artificially produced mesons showed that a large proportion of the negative mesons stopping in the emulsion gave rise to stars, while none of them appeared to disintegrate into secondary mesons. Of the positive mesons, instead, many ended in $\pi \to \mu$ processes while none gave rise to stars. These observations confirmed the early conclusion that only negatively charged mesons produce nuclear disintegrations after coming to rest. They also showed that artificially produced mesons must contain a much larger proportion of π-mesons than natural cosmic-ray mesons. Only in this way could one explain the fact that mesons giving rise to $\pi \to \mu$ decay processes were relatively so much more abundant among artificial mesons than among natural mesons.

In later experiments, measurement of range in the emulsion, accompanied by accurate grain counting on the meson tracks or by a determination of the radius of curvature of the mesons in the magnetic field of the cyclotron, afforded a clearer separation between π- and μ-mesons. Also, the introduction of a semicircular channel between the target and the plates made it possible to determine whether or not the observed mesons came from the target directly. The results obtained in these experiments may be summarized as follows:

(a) Both π- and μ-mesons arrive upon the photographic plates. Negative and positive π-mesons come directly from the target. Some of the positive μ-mesons come from the target, whereas none of the negative μ-mesons do. This is easily understandable if one assumes that π-mesons are the only product of the interaction between the α-particles and the target material. Positive π-mesons that come to rest in the target and subsequently decay are the source of the positive μ-mesons emanating from the target. Negative π-mesons, coming to rest in the target, however, undergo nuclear absorption before they have a chance to disintegrate.

Therefore the negative μ-mesons that arrive upon the photographic plates are all produced by π-mesons in flight and originate at some distance from the target.

(b) About 99 per cent of the positive π-mesons are seen to disintegrate into μ-mesons* after coming to rest in the emulsion. The difficulty of observing secondary μ-mesons traveling at a steep angle through the emulsion possibly accounts for the small number of events in which positive π-mesons appear to stop in the emulsion without giving rise to secondary particles. In any case, it is certain that, if any alternate disintegration process of π-mesons exists, it is improbable compared with the $\pi \to \mu$ decay.†

(c) About 73 per cent of the negative π-mesons give rise to stars at the end of their tracks in the emulsion (GE50). It appears likely that all negative π-mesons produce nuclear disintegrations after coming to rest in the emulsion but that in 27 per cent of the cases the nuclear disintegrations result in the emission of neutrons only.

(d) There is no evidence for the production of stars at the end of the tracks of negative μ-mesons. Thus star production by nuclear absorption of μ-mesons is at best a very rare event (see, however, § 4.12).

One should note that the emulsions used in the experiments described above were not sensitive to particles with minimum ionization. Therefore they could not provide information on the spontaneous decay of μ-mesons.

The significance of the striking difference between the effects of the nuclear absorption of negative π- and μ-mesons will be discussed later in some detail (§ 4.12). At this point we wish only to call attention to the fact that negative π-mesons appear always to undergo nuclear capture and never spontaneous decay after coming to rest in photographic emulsions. Since photographic emulsions contain light as well as heavy elements, this means that negative π-mesons are more likely to undergo nuclear absorption than spontaneous decay in all substances, whereas for negative μ-mesons this is true only in substances of high atomic number.

4.11. *The masses of the π-meson and the μ-meson.*‡ The following experiments have contributed most directly to our present knowledge of the masses of π- and μ-mesons.

(a) Momentum and range measurements on cosmic-ray mesons by Brode and his collaborators (FWB46; BRB49; RJG49; MTC50).§

(b) Momentum and range measurement on artificially produced mesons by the Berkeley group (VRL49; GE50; SFM50.2).

* Private communication from the Berkeley group to the author (December 1950).

† The possibility of the disintegration of a π-meson into an electron and a neutrino has been suggested on theoretical grounds (SL149.1; SL149.2). Friedman and Rainwater (FHL51), working with electron-sensitive emulsions, have claimed recently not to have observed any single case of π-e decay at the end of 829 tracks clearly recognizable as those of π-mesons. All of these tracks appeared to end in π-μ events. F. M. Smith (SFM51) has given a value of $(0.3 \pm 0.4) \cdot 10^{-2}$ for the ratio of π-e to π-μ decays.

‡ For a critical analysis of early mass determinations, see refs. (WJA41; BHA46).

§ A measurement based on a similar method has been described by Peyrou and Lagarrigue (PC50).

(c) Comparative measurements of grain density on the tracks of π- and μ-mesons by the Bristol group (LCM47.2; LCM48; BRH49.2) and on the tracks of mesons and protons by the Berkeley group (BJK50; BWH51).

(a) Figures 1 and 2 show schematically two of the experimental arrangements used by Brode and his collaborators. The first arrangement (RJG49, see Fig. 1) consists of two cloud chambers, CH_1 and CH_2. The upper chamber, CH_1, is placed in a magnetic field of 4,750 gauss produced

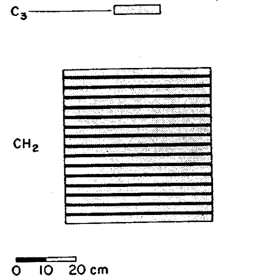

Fig. 4.11.1. Schematic arrangement of cloud chambers (CH_1, CH_2) and counters (C_1, C_2, C_3) used by Retallack and Brode for measuring the mass of cosmic-ray mesons (RJG49).

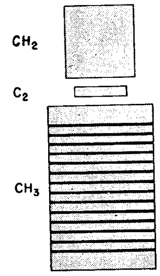

Fig. 4.11.2. Schematic arrangement of chambers, CH_1, CH_2, CH_3, counters, C_1, C_2, and magnet used by Brode and his collaborators for measuring the mass of cosmic-ray mesons (BRB49).

by an electromagnet. The lower chamber, CH_2, contains 15 lead plates 0.63 cm thick. The two chambers are triggered simultaneously whenever a charged particle passes through the Geiger-Mueller counters C_1, C_2, C_3, thus producing a threefold coincidence. The curvature of the track in the upper chamber determines the momentum of the particle. When the particle stops in the lower chamber, observation of the plate in which the track ends determines the range. Knowledge of momentum and range yields the mass of the particle.

The second arrangement (BRB49; see Fig. 2) consists of three cloud chambers, triggered by the coincidences of two Geiger-Mueller counters placed, respectively, above the top chamber and between the middle chamber and the bottom chamber. Between the top chamber and the middle chamber the particles pass through the gap in a permanent magnet producing a field of about 5,000 gauss. The momentum of a particle is determined by the angle between the directions of its trajectory in the upper and in the middle chamber respectively. Its range is determined in the bottom chamber containing 13 lead plates, each 0.6 cm thick.

If one assumes, in each case, that the stopping point of the meson is at the center of the plate where the trajectory ends, the limiting error in the determination of the range equals one-half the thickness of the plate divided by the cosine of the angle of incidence. The error in the measurement of the momentum results partly from scattering, partly from instrumental distortions (§ 3.13). From the computed values of these two errors, one may estimate the error in the individual mass determinations. For the best experiments, the probable error turns out to be about 12 per cent. However, it is likely that uncontrollable factors often introduce considerably larger errors.

Histograms showing some of the experimental results obtained by Brode and his collaborators are reproduced in Fig. 3. Most of the experimental data are grouped around a mass value of about 200 electron masses. The small number of observations lying outside of the main group may be explained by instrumental errors and cannot be taken as a proof for the existence of mesons with anomalous masses. In a private communication to the writer (October 1950), Robert Brode indicated the figure of 206 electron masses (with a probable error of 2) as the best value for the meson mass obtained from his measurements and those of his collaborators. This figure is based upon the assumption that all mesons observed have the same mass. At sea level, where the observations were made, almost all cosmic-ray mesons are μ-mesons, the average mass value, therefore, must come very close to the mass of these particles. It is true that the accuracy of the individual measurements was not sufficient to detect the possible presence of a small number of π-mesons. However, the error in the average mass value due to the inclusion of these particles is probably small compared with the other experimental errors.

(b) The mass measurements on artificially produced mesons were made with experimental arrangements of the type shown in Figs. 4.10.2 and 4.10.3. With these arrangements one observes mesons emitted from the target and entering the emulsion on the edge of the plates after describing part of a circular path in the magnetic field of the cyclotron. The point of incidence and the direction of the track when it first enters the emulsion determine the radius of curvature of the path in the magnetic field and therefore the momentum. When the particle comes to rest in the emulsion, the total length of its track determines the range. From the values of momentum and range one computes the mass. The method described can be applied to the measurement of the masses of positive π-mesons, negative π-mesons, and positive μ-mesons (there are no negative μ-mesons

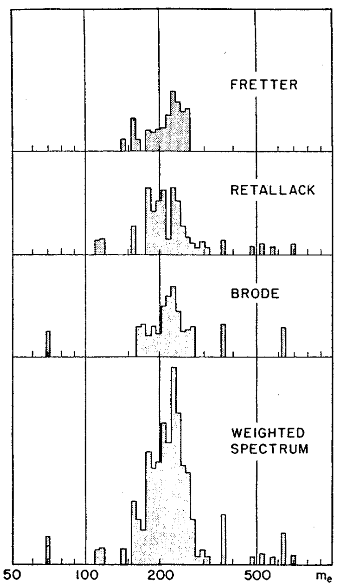

Fig. 4.11.3. Mass spectra of cosmic-ray mesons obtained by Brode and his collaborators (BRB49).

coming from the target). To achieve more accurate results the authors did not trust the momentum-range relation obtained with independent measurements, but compared, in the same emulsions, the ranges of protons and mesons of approximately equal velocities.

The mass values determined by this method were (SFM50.2; BWH51):

$$\text{positive } \pi\text{-mesons: } m_\pi = (277.4 \pm 1.1)m_e,$$

$$\text{negative } \pi\text{-mesons: } m_\pi = (276.1 \pm 1.3)m_e,$$

$$\text{positive } \mu\text{-mesons: } m_\mu = (210 \pm 4)m_e.$$

(c) Measurements of mass ratios from range and grain density (§ 3.16) were reported by the Bristol and the Berkeley groups. The Bristol group

used this method for comparing the masses of π- and μ-mesons associated in $\pi \rightarrow \mu$ disintegration processes (see Fig. 4.8.1). Measurements of this kind can yield fairly accurate results, provided one considers only those events in which the π-meson track is sufficiently long. The fact that the two tracks to be compared are produced practically at the same time and in the same region of the emulsion eliminates any possible error due to fading or to lack of homogeneity of the emulsion. Early experiments, made in part on π-meson tracks not very suitable for grain counting, gave a value $m_\pi/m_\mu = 1.65$ for the mass ratio of π- and μ-mesons (LCM48). Later experiments (BRH49.2), in which a more rigorous selection of the pictures was made, gave $m_\pi/m_\mu = 1.33 \pm 0.05$ in good agreement with the results described above.

The Berkeley group used the grain-counting method to compare the masses of π- and μ-mesons with the mass of the protons. Measurements by Bowker (BJK50) on positive π-mesons gave $m_\pi = 264(^{+26}_{-22})$ electron masses.

4.12. ***Products of the nuclear absorption of negative π-mesons and μ-mesons.*** We have mentioned repeatedly that most of the negative π-mesons that come to rest in photographic emulsions produce nuclear stars at the end of their tracks. The nuclear explosions responsible for the observed stars require energies of the order of 100 Mev, i.e., of the same order of magnitude as the rest energy of π-mesons (140 Mev).

These observations can be interpreted easily if one assumes that when a negative π-meson is absorbed by a nucleus, it combines with one of the protons in the nucleus, changing the proton into a neutron:

$$\pi^- + p \rightarrow n. \tag{1}$$

Since the rest energies of the proton and the neutron are nearly equal, the reaction considered here releases an amount of energy practically equal to the rest energy of the π-meson.

Note that the process described by Eq. (1) cannot conserve energy and momentum without the participation of other particles. Therefore it cannot take place if the proton is free, but only if the proton is bound to a nucleus, so that other nucleons may participate in the interaction and insure the momentum balance.* It follows that the neutron resulting directly from the absorption of the meson does not acquire all of the energy released by the disappearance of the meson, even though, under favorable conditions, it may acquire a large fraction of it.

In any case the absorption of a negative π-meson by a nucleus causes a small number of nucleons in the nucleus to acquire kinetic energies totalling 140 Mev. Usually these nucleons will collide with other nucleons, distributing most of their energy among them and thus giving rise to a

* The nuclear absorption of μ-mesons in hydrogen will be discussed separately in §4.16.

violent nuclear explosion. Occasionally, however, they may escape from the nucleus without further collision, leaving the nucleus in a mildly excited state. In § 4.10 we have mentioned that about 27 per cent of the negative π-mesons fail to produce visible stars at the end of their tracks in Ilford C2 emulsions. In these cases, presumably, the energy released by the disappearance of the π-meson is carried away by neutrons [perhaps, to a large extent, by the neutron resulting directly from the interaction described by Eq. (1)], or by protons of energy greater than the maximum energy detected by electron-insensitive emulsions.

The study of the absorption of negative π-mesons by nuclei is one of great interest in connection with the problem of the nuclear structure. However, a detailed discussion of this phenomenon goes beyond the limits of the present volume, whose main objective is a description of the properties of elementary particles. We wish only to mention some of the results obtained by Menon, Muirhead, and Rochat (MNG50) with photographic emulsions.

These authors examined 1337 nuclear stars caused by artificially produced π-mesons and 1216 nuclear stars caused by natural π^--mesons. They used the following methods for separating the disintegrations of the heavy nuclei (Br,Ag) and of the light nuclei (C,N,O) contained in the emulsion:

(1) Observations with "sandwich plates," i.e., plates covered with alternate layers of normal emulsion and of pure gelatine (containing only light elements);

(2) Energy measurements on the α-particles occurring in nuclear stars; α-particles of energy appreciably smaller than the potential barrier of bromine must arise from the light nuclei;

(3) Observations on the occurrence of low-energy electrons in nuclear stars; these electrons (which can be detected only in electron-sensitive emulsions) are explained as the result of an Auger effect that takes place when a π-meson is captured by a heavy nucleus.

The three methods described above gave mutually consistent results. They showed that in normal nuclear emulsions 46 $\pm$ 5 per cent of the stars due to the capture of π^--mesons correspond to the disintegration of light nuclei, 54 $\pm$ 5 per cent correspond to the disintegration of heavy nuclei. Table 1 gives the distribution of stars according to number of prongs, for stars originating in light and heavy nuclei separately as well as for all stars. In agreement with previous results (§ 4.10), the number of π^--mesons that come to rest in the emulsion without giving rise to visible stars was found to be 28 $\pm$ 2 per cent.

The results of Menon and his collaborators, in agreement with those of Cheston and Goldfarb (CWB50), showed that about 10 per cent of the π^--mesons ending in the emulsion give rise to protons with energies greater than 30 Mev. Among these, some have energies as high as 80 Mev.

Table 4.12.1. The percentage of stars with different numbers of prongs produced by the absorption of π^--mesons in the light (*L*) and in the heavy (*H*) nuclei present in photographic emulsions. [Not considered here are those absorption processes of π^--mesons that do not give rise to visible stars (28 $\pm$ 2 per cent of the total).] From Menon *et al.* (MNG50).

Number of Prongs	Number of Stars L	H	L + H
1	11	27	37
2	13	18	31
3	15	4	20
4	6	4	10
5	1	1	2
6	—	—	—
Totals:	46	54	100

The existence of protons with such large energies is a direct proof that a large fraction of the rest energy of the π^--meson goes into a single nucleon, and thus confirms the assumption about the mode of π^--capture expressed by Eq. (1).

Negative μ-mesons behave very differently from negative π-mesons when absorbed by atomic nuclei. This fact was first indicated by the experiments of Lattes, Occhialini, and Powell (LGM47.4) already mentioned in § 4.9. In Ilford C2 emulsions exposed to the cosmic radiation, these observers found that the number of mesons either ending in stars or giving rise to secondary mesons was a very small fraction of the number of those that did not produce any visible event at the end of their range. Most of the mesons stopping in the emulsion were, of course, μ-mesons. Since the emulsion used in these experiments was insensitive to electrons, it could not detect the spontaneous decay of positive μ-mesons. However, about half of the μ-mesons coming to rest in the emulsion were negative μ-mesons and many of them were certainly absorbed by the heavy nuclei of the emulsion (silver, bromine). If most of these mesons had given rise to stars (as π^--mesons do), the relative number of meson tracks ending in stars should have been much greater than was actually observed.

The above results were later confirmed by the observations on the behavior of artificially produced mesons described in § 4.10. They were also confirmed by cloud-chamber experiments showing that μ-mesons often stop without giving rise to either decay electrons or ionizing nuclear fragments.*

Wang and Jones (WKC48), for example, working with a cloud chamber containing two lead plates, each 0.63 cm thick, and five aluminum foils,

* For a review of experimental evidence on this subject prior to 1948, see ref. (PO48.1).

0.08 cm thick, observed 20 mesons stopping in lead and 20 mesons stopping in aluminum. In 19 cases they detected a lightly ionizing particle, presumably a decay electron, coming out of the absorber in which the meson had stopped. There was one event that could be interpreted either as a meson stopping in an aluminum foil and giving rise to a low-energy proton, or as a meson undergoing a large-angle scattering in an aluminum foil and emerging from it with very small velocity. In all other cases there was no evidence for the emission of ionizing particles from the end of the meson track.

In a similar experiment Chang (CWY49) observed 45 mesons stopping in thin metal foils inside a cloud chamber without giving rise to visible secondary events of any kind. During the same experiment he also obtained 26 pictures of decay processes and one picture that appeared to show a meson stopping in a foil and producing a single low-energy proton by a nuclear interaction. However, the interpretation of this picture is not entirely unambiguous, according to the author.*

In the same connection one may also mention the results of some experiments by Voorhies and Street (VHG49) on μ-mesons stopping in a crystal of silver chloride. Under appropriate conditions, such a crystal operates as a "solid" ionization chamber and is thus capable of detecting whatever heavily ionizing particles may be emitted by the nuclear absorption of negative μ-mesons. The result of this experiment was negative, again showing that most negative μ-mesons do not produce ionizing secondary particles when absorbed by nuclei.

In contrast, but not in contradiction with the experiments described above, recent observations of George and Evans (GEP51) have shown that a *small fraction* of the μ-mesons coming to rest in photographic emulsions do give rise to visible stars. These workers used Ilford G5 electron-sensitive emulsions prepared, stored, and developed underground, at depths of 2000, 3400, and 6000 g cm^{-2} below sea level. The number of π-mesons, relative to that of μ-mesons, is much smaller underground than above ground. This is so because, in cosmic rays, short-lived π-mesons arise from locally produced nuclear interactions whose rate of occurrence decreases with increasing depth much more rapidly than the intensity of μ-mesons (§ 8.4). Therefore, if any stars are produced by the nuclear absorption of μ mesons, they can be detected more easily underground, where the background due to π^--mesons is smaller than above ground.

In an examination of their plates, George and Evans found 1014 μ-mesons ending in the emulsion without producing visible disintegrations, 5 π-mesons showing $\pi \rightarrow \mu$ decay processes, and 30 mesons producing stars at the end of their tracks. The following arguments prove that most

* On the subject of cloud-chamber observations on mesons at the end of their range, see also (CRI49).

of the 30 star-producing mesons are negative μ-mesons and not negative π-mesons.

(a) The number-prong distribution of the stars observed underground is very different from that of the stars observed above ground and shows a much larger proportion of stars with small numbers of prongs.

(b) The number of star-producing mesons is much greater than the number of mesons giving rise to $\pi \rightarrow \mu$ decay processes.

(c) The 30 star-producing mesons like the 1014 μ-mesons ending uneventfully are strongly collimated around the vertical, whereas the mesons giving rise to $\pi \rightarrow \mu$ decays are distributed nearly isotropically.

George and Evans tentatively identified 5 of the 30 star-producing mesons as negative π-mesons and the remaining 25 as negative μ-mesons. Of these, 3 produced 2-pronged stars and 22 produced 1-pronged stars. George and Evans further estimated that 265 negative μ-mesons had undergone nuclear absorption without producing visible stars. They arrived at this conclusion by considering the total number of μ-mesons ending in the emulsion, by assuming a value of 1.27 for the ratio of positive to negative μ-mesons, and by taking into account the fact that negative mesons captured in Ag or Br mostly undergo nuclear absorption whereas those captured by C, N, O, and H mostly undergo spontaneous decay. Table 2 shows the distribution in number of prongs for stars due to nuclear absorption of negative μ-mesons, according to George and Evans.

Table 4.12.2. The number of stars with different numbers of prongs produced by the absorption of μ^--mesons in the heavy nuclei present in photographic emulsions (μ^--mesons are not appreciably absorbed by light nuclei).
From George and Evans (GEP51).

Number of prongs	0	1	2	$\geqslant 3$
Number of stars	265	22	3	0

The difference between the distributions shown in Tables 1 and 2, respectively, is very marked. One may add that most of the star particles produced by the nuclear absorption of μ^--mesons have small energies, of the order of several Mev.

Before any clear evidence for the occasional production of stars by the nuclear absorption of negative μ-mesons was available, Piccioni carried out an experiment to investigate whether or not *high-energy photons* are produced when μ-mesons stop in iron (PO48.2). The result was negative, indicating, according to an estimate of the author, that the average energy emitted in the form of γ-rays is less than 20 Mev per negative μ-meson absorbed in iron.

Also, several experimenters investigated the possibility that *neutrons* be produced by the nuclear absorption of negative μ-mesons. Sard and his collaborators (SRD48.2; SRD49) used for this purpose the experimental arrangement shown in Fig. 1, which is designed to detect neutrons associated with the stopping of ionizing particles in lead. A, B, and C are trays of Geiger-Mueller counters. N are proportional counters coated on the inside with boron enriched in B^{10} (§ 3.4). They are embedded in a large paraffin block, which brings moderately fast neutrons down to thermal or epithermal energies, where they are effectively detected by the boron counters. Ionizing particles stopping in the lead absorber between B and C give rise to anti-coincidences ($AB - C$). Each anti-coincidence initiates, with a 4-microsecond delay, an 80-microsecond square pulse ("gate"), which is placed in coincidence with the pulses of the neutron detectors. Neutrons originating in the lead absorber and entering the paraffin block take several microseconds to reach thermal velocity, and the mean life of the thermal neutrons in a paraffin block of the dimensions shown in Fig. 1 is of the order of 150 microseconds. Therefore the late start of the "gate" does not result in an appreciable loss of counts for the phenomenon under investigation, while it eliminates a number of spurious effects.

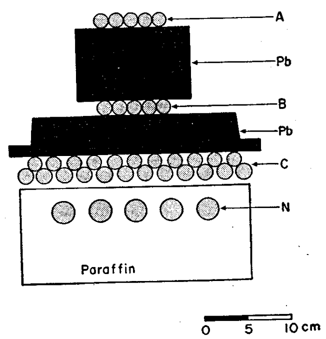

Fig. 4.12.1. Experimental arrangement used by Sard *et al.* to investigate the production of neutrons by stopping of mesons in lead (SRD48.2).

In 181 hours of operation the instrument recorded 61 coincidences between ($AB - C$) events and neutron pulses [events ($AB - C{:}N$)]. No such coincidence was recorded in 50 hours of operation when the neutron counters were surrounded by a 1-mm-thick cadmium shield (which is completely opaque to slow neutrons). This result showed that the observed effect was actually caused by neutrons. In another test run, Sard and his collaborators removed the high voltage from the anti-coincidence counters so as to make them inoperative and found that the counting rate of the cosmic-ray telescope increased by a factor of 30 while the rate of ($AB - C{:}N$) events increased only by a factor of two. This result proved that the ($AB - C{:}N$) events recorded with the anti coincidence counters in operation were not caused, to any appreciable extent, by secondary effects of penetrating particles that traversed the lead absorber between B and C but failed to discharge tray C. Thus the experiment described gave convincing evidence for the production of neutrons by the stopping of ionizing particles in lead. These neutrons had energies of less than about 10 Mev, for the thickness of the paraffin block was not sufficient to slow down to thermal velocities neutrons of substantially higher energies.

It was still necessary to investigate whether or not the particles giving rise to neutrons at the end of their range were actually μ-mesons. One had, indeed, to consider the possibility of neutron production by nuclear interactions of protons; for proton energies up to several hundred Mev, the secondary ionizing products of the interaction have a very short range and a correspondingly small probability of emerging from the lead absorber.

One can distinguish between the effects of μ-mesons and protons by means of underground measurements, because the number of protons decreases with increasing depth much more rapidly than the number of slow μ-mesons (see § 8.4). In this manner Sard and his collaborators were able to show that about one-half of the ($AB - C{:}N$) events observed at sea level were actually due to nuclear absorption of negative μ-mesons (SRD51). They also found that, on the average, the absorption of a negative μ-meson by a lead nucleus is followed by the emission of 2 neutrons with energies between 0.1 and 10 Mev [see also (GG51)].

Groetzinger and his collaborators (GG48; MGW49) confirmed the experimental results obtained by Sard's group. Moreover, they provided a final check of their interpretation by separating negative from positive mesons magnetically and showing that only the former produce neutrons after coming to rest in matter.

In conclusion, the available experimental data prove that negative μ-mesons, when absorbed by nuclei, do not produce violent disintegrations comparable to those following the absorption of negative π-mesons. A nucleus that has absorbed a μ-meson emits ordinarily only a few neutrons of several Mev energy, more seldom a proton of equally low energy, and very rarely more than one ionizing particle. In all cases the total energy of the disintegration products is a small fraction of the rest energy of μ-mesons.

This behavior, which is so strikingly different from the behavior of negative π-mesons, can be understood only if one assumes that the nuclear absorption of negative μ-mesons brings the nucleus into an excited state not more than 10 or 20 Mev above the ground level. As noted by Wheeler (WJA49), an excitation energy of this order of magnitude is much more likely to produce the emission of neutrons than the emission of protons, especially in elements of large atomic number in which the "Coulomb barrier" is high. (And, of course, in elements of small atomic number negative μ-mesons have a small probability of undergoing nuclear absorption.) The above assumption, however, means that a comparatively small portion of the rest energy of negative μ-mesons goes into excitation of the nucleus. This would be difficult to understand if the direct result of the absorption of a negative μ-meson by a nucleus was the transformation of a proton into a neutron according to the reaction:

$$\mu^- + p \rightarrow n.$$

The most natural interpretation of the observed behavior lies in the assumption that the interaction of the negative μ-meson with the proton gives rise to a neutron plus a neutrino:*

$$\mu^- + p \rightarrow n + \nu. \tag{2}$$

In this case it can be shown, on general theoretical grounds, that the neutrino almost always takes a large part of the energy set free by the disappearance of the meson, leaving a small fraction available for the excitation of the nucleus.

Insofar as the properties of elementary particles are concerned, the most important result of the experiments described in the present section is the evidence in favor of the interactions represented symbolically by Eqs. (1) and (2). From the character of these interactions one can draw some important conclusions regarding the spin of π- and μ-mesons. Since both the proton and the neutron have spin $\frac{1}{2}$, Eq. (1) shows that the π-meson must have integer spin. Since, moreover, the neutrino has spin $\frac{1}{2}$, Eq. (2) shows that the μ meson must have half-integer spin. Experimental results to be described in §§ 4.13, 4.15, and 4.16 supply corroborating evidence in favor of the above conclusions and show that the spin of the π-meson is probably zero. As for the spin of the μ-meson, it is simplest to assume that it has the value $\frac{1}{2}$. One could test this assumption experimentally by measuring the collision and radiation probabilities of high-energy μ-mesons. As shown in §§ 2.3 and 2.14, these probabilities are much greater for particles of spin $\frac{3}{2}$ than for particles of spin $\frac{1}{2}$. Some experiments that have a bearing upon this question will be discussed in § 6.13.

4.13. *Disintegration products of π-mesons and μ-mesons.* The observations by means of cloud chambers and photographic emulsions

* This process was first suggested by Sakata and Inoue (SS46). For a discussion of the experimental evidence, see also (PDH49).

described in §§ 4.7 and 4.8 show that when a π- or a μ-meson disintegrates, only one charged particle is emitted in each case. When the disintegrating particle is a π-meson the secondary particle is a μ-meson; when the disintegrating particle is a μ-meson the secondary particle is an electron.

The principles of conservation of energy and momentum, however, require that two or more particles be produced when a meson disappears, so that, in the frame of reference in which the meson is at rest, the momenta of the disintegration products may cancel vectorially while their energies add up to the rest energy of the original meson. Therefore the disintegration of both the π- and the μ-meson must be accompanied by the emission of one or more neutral particles.

If there is only one neutral particle, this and the charged particle must carry equal and opposite momenta in the frame of reference of the original meson. Therefore the charged particle arising from the disintegration of a meson at rest will always have the same kinetic energy, E_1. The conservation principles yield for this energy the following value:

$$E_1 = \frac{(mc^2 - m_1c^2)^2 - (m_0c^2)^2}{2mc^2}, \tag{1}$$

where m is the mass of the primary particle, m_1 is the mass of the secondary charged particle, and m_0 is the mass of the secondary neutral particle.

If there are two or more neutral particles arising from the disintegration process, then the energy, E_1, of the secondary charged particle is not determined. In this case one should expect a continuous distribution of values for this energy, from zero to a certain maximum, as in the case of the β-decay (§ 4.5). E_1 is a maximum when all of the secondary neutral particles are emitted in the same direction, opposite to the direction of emission of the charged particle, and with the same velocity. This maximum value is given by Eq. (1), where m_0 now represents the sum of the masses of all the neutral particles.

Consider first the case of the $\pi \rightarrow \mu$ decay. Experiments by the Bristol group (LCM47.2), later confirmed by those of the Berkeley group (BJ49), showed that the ranges in the emulsion of the secondary μ-mesons are dis-

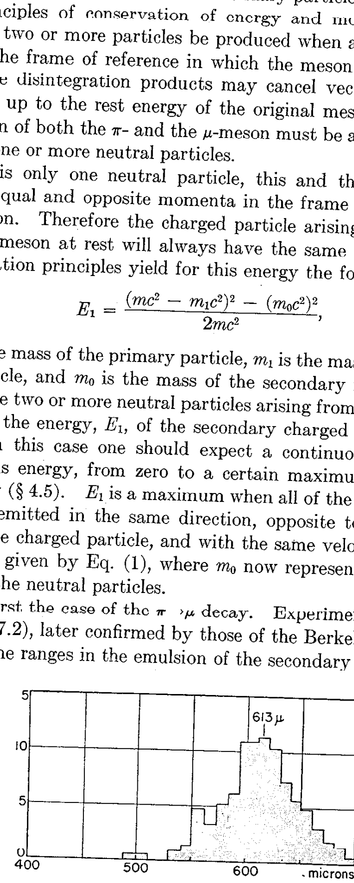

Fig. 4.13.1. Distribution in range of the μ-mesons produced by the spontaneous decay of π-mesons at rest, as observed in Ilford C2 emulsion. From C. F. Powell (PCF49).

tributed over a very narrow interval. This is illustrated by the histogram in Fig. 1, taken from a paper by Powell (PCF49). In fact, the observed spread in range can be fully explained by straggling (§ 2.8) under the assumption that the μ-mesons arising from the disintegration of π-mesons at rest all have the same kinetic energy. According to the data summarized in Fig. 1, the average range in the emulsion is 613 microns; the corresponding kinetic energy (see Fig. 3.15.2) is:

$$E_1 = 4.17 \pm 0.06 \text{ Mev}. \tag{2}$$

Note that since the energy-range relation is insensitive to the mass of the particle, the experimental uncertainty in the mass of μ-mesons (see § 4.11) does not affect the value of E_1 appreciably.

The fact that the secondary μ-mesons all have the same energy shows that the $\pi \rightarrow \mu$ disintegration process gives rise to one and only one neutral particle. One can use Eq. (1) and the experimental values of E_1, $m(= m_\pi)$ and $m_1(= m_\mu)$ to compute the mass, m_0, of this neutral particle. One finds that m_0 is small compared with the mass of μ-mesons and could be zero within the experimental error. One can easily show that the assumption $m_0 = 0$ is consistent with the experimental results, by computing E_1 from Eq. (1) under this assumption. With $m = m_\pi = 276$ (from the Berkeley measurements on artificial mesons; § 4.11) and $m_1 = m_\mu = 206$ (from Brode's measurements on cosmic-ray mesons; § 4.11), one obtains: $E_1 = 4.5$ Mev. This value agrees with that obtained from direct measurement, within the experimental uncertainties of the two values.

In conclusion, the experimental values of E_1, m_π, and m_μ indicate that the neutral particle produced simultaneously with the μ-meson when a π-meson decays is either a neutrino or a photon. On the other hand, in § 4.12 we have shown that π-mesons have integer spin and μ-mesons have half-integer spin. Conservation of spin then assigns half-integer spin to the neutral disintegration product of a π-meson and therefore shows that this particle is a neutrino. The disintegration of a π-meson is thus represented schematically by the following equation:

$$\pi^\pm \rightarrow \mu^\pm + \nu. \tag{3}$$

If our conclusions are correct, the true values of m_π, m_μ, and E_1 are related by the equation obtained from Eq. (1) with the substitutions: $m = m_\pi$, $m_1 = m_\mu$, $m_0 = 0$. We shall adopt in our discussion the following values:

$$\left.\begin{aligned} &m_\pi = 276 m_e; \quad m_\mu = 209 m_e; \quad E_1 = 4.18 \text{ Mev};\\ &m_\pi c^2 = 1.41 \cdot 10^8 \text{ ev}; \quad m_\mu c^2 = 1.07 \cdot 10^8 \text{ ev};\\ &\frac{m_\pi}{m_\mu} = 1.32. \end{aligned}\right\} \tag{4}$$

These values satisfy the condition specified above and are consistent with the experimental determinations, within the probable errors of the latter.

We next turn our attention to the decay of μ-mesons into electrons. Measurements on the energy distribution of the decay electrons have been reported by Leighton, Anderson, and Seriff (LRB49).* These experimenters used an ingenious device, originally suggested by Wilson and Wilson (WCT35), i.e., a cloud chamber placed between the pole pieces of an electromagnet, which is allowed to fall freely after the expansion has taken place and is photographed some distance below the magnet. This type of cloud chamber eliminates the need of a mirror in the magnet gap or of a hole in the magnet core (§ 3.13) and thus simplifies the problem of obtaining a strong and uniform magnetic field. Note that the accelerated motion of the chamber during the free fall effectively removes gravitational forces and, therefore, eliminates track distortions arising from the free fall of the droplets and from convection currents in the gas.

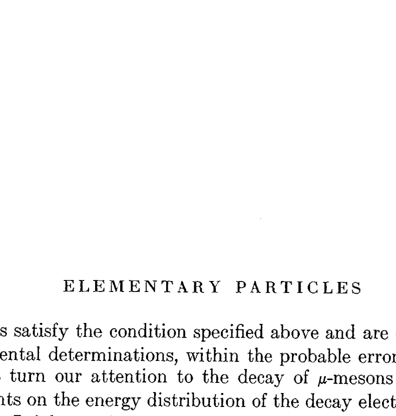

Fig. 4.13.2. Schematic diagram of cloud chamber and counters used by R. B. Leighton *et al.* for the measurement of the spectrum of decay electrons (LRB49). *P* is a carbon plate: C_2 is a Geiger-Mueller tube whose sensitive volume is represented by the shaded portion.

The experimental arrangement is shown schematically in Fig. 2. The cloud chamber contains a carbon plate, P, 2.0 g cm^{-2} in thickness and a Geiger-Mueller counter, C_2, whose outer envelope consists of a square copper box of 0.87 mm wall thickness. The chamber is triggered by those simultaneous pulses of this counter and of the upper counter tray, C_1, that are not accompanied by pulses of the lower counter tray, C_3 (anti-

* For a discussion of earlier measurements see ref. (RB49).

coincidences $C_1C_2 - C_3$). This method of triggering favors the recording of "slow" μ-mesons.

Out of a total of 15,000 photographs obtained in a 7250-gauss magnetic field, 75 showed mesons that stopped either in the gas, in the wall of counter C_2, in the carbon plate, or in the walls of the chamber and gave rise to secondary electrons whose energy could be determined. The energy distribution of these 75 electrons is shown in Fig. 3. The estimated error

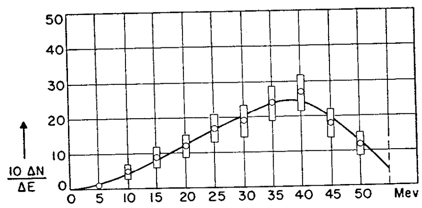

Fig. 4.13.3. Differential energy spectrum of electrons arising from the decay of μ-mesons. Each point represents the number of electrons per energy interval of 10 Mev. Standard statistical errors are indicated. From Leighton *et al.* (LRB49).

in the individual energy measurements is between 1 and 2 Mev. Figure 3 clearly demonstrates that the electrons arising from the decay of μ-mesons do not have a unique energy. From the arguments developed above, it then follows that *two or more neutral particles originate from the decay of each μ-meson.* The maximum energy of the decay electron is:

$$E_1 = 55 \pm 1 \text{ Mev}. \tag{5}$$

This result together with Eq. (1) shows that the total mass of the neutral particles is small compared with the mass of μ-mesons and could be zero within the experimental errors. In fact, Eq. (1) with $m = m_\mu = 209m_e$, $m_1 = m_e$, and $m_0 = 0$ gives $E_1 = 53$ Mev, which comes close to the experimental value.

Several experimenters investigated the possibility that the neutral disintegration products of the μ-meson may be photons (SRD48.1; HEP48; PO48.2). The results of these experiments were negative.* It thus appears likely that the neutral disintegration products are neutrinos. The simplest assumption is that each μ-meson disintegrates into one electron and two neutrinos:

$$\mu^\pm \rightarrow e^\pm + \nu + \nu. \tag{6}$$

* We may add that measurements on the relative numbers of electrons and mesons in the atmosphere near sea level also rule out the possibility that photons are produced by the decay of μ-mesons (GKI43).

The maximum of the energy spectrum occurs around 40 Mev. The measured average energy of the decay electrons is 34 Mev, which comes close to one-third of the rest energy of the μ-meson. This would indicate, that, on the average, the energy of the disintegrating μ-meson is divided equally among the three disintegration particles.†

One particularly interesting picture obtained in the experiment just described shows a decay particle deflected by the magnetic field in such a way as to traverse four times the carbon plate before coming to rest within the plate. The values of the momentum of this particle after each traversal were measured. From the momentum losses thus determined, as well as from an estimate of the specific ionization toward the end of the path, the authors were able to place an upper limit of $10m_e$ to the mass of the decay particle. This is perhaps the clearest piece of experimental evidence so far available in support of the assumption that the charged particles produced by the decay of μ-mesons are indeed electrons.‡

The disintegration scheme of μ-mesons represented by Eq. (6) confirms the conclusion concerning the spin of μ-mesons reached in § 4.12. Indeed, since electrons and neutrinos have spin $\frac{1}{2}$, the finding that one electron and two neutrinos arise from the decay of each μ-meson shows that μ-mesons have half-integer spin.

The discussion in this section has centered in the disintegration of mesons at rest. For future reference, we develop here some relations concerning the decay of mesons in flight.

Consider first the case of a two-particle disintegration. Let m be the mass of the primary particle, m_1 that of one of its disintegration products. The total energy and the momentum of the secondary particle in the frame of reference in which the primary particle is at rest have constant values, that will be called U_1^* and p_1^* respectively. In the same frame of reference, let θ^* be the angle of emission of the secondary particle measured from the trajectory of the primary particle. In the laboratory system, let U, p, and β be the total energy, the momentum and the velocity of the primary particle; let U_1 and p_1 be the total energy and the momentum of the secondary particle. The Lorentz transformation yields:

$$U_1 = \frac{U_1^* + \beta c p_1^* \cos\theta^*}{\sqrt{1-\beta^2}} = \frac{U}{mc^2} U_1^* + \frac{p}{m} p_1^* \cos\theta^*, \tag{7}$$

from which one obtains:

$$\begin{aligned} (U_1)_{\min} &= \frac{U_1^* - \beta c p_1^*}{\sqrt{1-\beta^2}} = \frac{U}{mc^2} U_1^* - \frac{p}{m} p_1^*, \\ (U_1)_{\max} &= \frac{U_1^* + \beta c p_1^*}{\sqrt{1-\beta^2}} = \frac{U}{mc^2} U_1^* + \frac{p}{m} p_1^*. \end{aligned} \tag{8}$$

† Further experimental data on the energy spectrum of electrons arising from the decay of μ-mesons will be found in refs. (SgR51) and (BrH51). The effect of Bohr orbit binding on the decay spectrum of negative μ-mesons has been computed by Porter and Primakoff (PCE51).

‡ On this subject, see also ref. (HEP50).

In the frame of reference of the primary particle, the probability of emission of the secondary particle is the same in all directions. Therefore the average value of $\cos\theta^*$ is zero and the average value of U_1 is given by the following equation:

$$\langle U_1\rangle_{av} = \frac{U_1^*}{\sqrt{1-\beta^2}} = \frac{U}{mc^2}U_1^*. \tag{9}$$

The fractional number, dn, of secondary particles emitted at an angle between θ^* and $\theta^* + d\theta^*$ in the frame of the primary particle is:

$$dn = \tfrac{1}{2}\sin\theta^*\,d\theta^*. \tag{10}$$

In the laboratory system, the energy of these particles lies in the interval between U_1 and $U_1 + dU_1$ where θ^* and U_1 are related by Eq. (7). Differentiation of this equation yields, in absolute value:

$$dU_1 = \frac{p}{m}p_1^*\sin\theta^*\,d\theta^*, \tag{11}$$

which, together with Eq. (10), gives:

$$dn = \frac{1}{2}\frac{m}{p}\frac{dU_1}{p_1^*}. \tag{12}$$

Thus, in the case of a two-particle disintegration, the differential energy spectrum for each secondary particle has a constant value between the limits $(U_1)_{min}$ and $(U_1)_{max}$ given by Eqs. (8).

If the disintegration particles are more than two, then U_1^* and p_1^* are not constant. However, Eq. (9) still holds, provided U_1^* is interpreted as the average energy of the secondary particles of a given kind in the frame of reference of the primary particle.

4.14. ***The mean life of π-mesons.*** Independent and practically simultaneous experiments by Camerini, Muirhead, Powell, and Ritson (CU48) with cosmic-ray mesons and by Richardson (RJR48) with artificially produced mesons provided the first direct, even though crude, estimates of the mean life of π-mesons.†

Camerini and his collaborators exposed a stack of photographic plates to cosmic rays at 3450 meters altitude. The plates were suspended under a light roof, 2 meters above a concrete floor, with the emulsions in a vertical plane. Of the mesons ending in the emulsions, most came from above, some, however, from below. The latter, presumably, were mesons projected upward by nuclear interactions occurring in the matter beneath the plates. In the upward stream of mesons, both π- and μ-mesons were present in comparable numbers. If one assumes that only π-mesons are produced in nuclear interactions, the μ-mesons must arise from the decay of π-mesons in flight. From the measured relative abundances of π- and μ-mesons in the upward stream, and from an estimate of the mean distance from the plates of the point of origin of mesons, one can then roughly evaluate the mean life of π-mesons. The value thus obtained was:

$$\tau_\pi \approx 0.6 \cdot 10^{-8}\text{ sec.}$$

† For previous indirect estimates of this quantity, see refs. (MRE47) and (GKI48).

Richardson used as source of π-mesons a thin graphite target placed in the internal α-ray beam of the Berkeley cyclotron. The α-ray beam is in a horizontal plane. In the magnetic field of the cyclotron, the mesons spiral upward or downward depending on the direction of emission. Richardson selected an upward-spiralling group of mesons by means of a semi-circular helical channel that rose 1.25 cm vertically in one semicircle (180°). At the end of the channel he placed six photographic plates. He also selected a group of mesons spiralling downward by means of a similar helical channel, which, however, extended for one and one-half circles (540°). At the end of this second channel he placed another stack of photographic plates. The ratio of the numbers of mesons found in the two sets of plates, when corrected for geometry, gives the loss of mesons by decay in the time corresponding to one revolution in the magnetic field.

If $\mathcal{B}$ is the magnetic induction, p the momentum of the mesons, and θ the angle between their trajectory and the magnetic field, the radius of the spiral orbit is:

$$R = \frac{pc}{e\mathcal{B}}\sin\theta.$$

On the other hand, the mean path length before decay for a π-meson of momentum p, from Eq. (4.7.1), is $z_d = p\tau_\pi/m_\pi$. Therefore the survival probability after one revolution is:

$$w = \exp\left(-\frac{2\pi R}{z_d\sin\theta}\right) = \exp\left(-\frac{2\pi m_\pi c}{e\mathcal{B}\tau_\pi}\right). \tag{1}$$

One sees that the survival probability is independent of the momentum of the mesons and is a function of the ratio of their mean life to their mass.

With the experiments described above, Richardson found the following value for the mean life of the *negative* π-meson:

$$\tau_\pi = (1.1\,^{+0.31}_{-0.22}) \cdot 10^{-8}\text{ sec.} \tag{2}$$

Later Martinelli and Panofsky (MEA50) used a similar method for determining the mean life of *positive* π-mesons. They achieved greater accuracy by using a stronger source of mesons and by taking two points instead of one on the decay curve. For this purpose they selected the downward-spiralling mesons with a channel extending over two and one-half turns and made measurements with photographic plates placed at either 540° or 900° in this channel. In the upper channel the plates were always placed at 180°. The value of the mean life obtained by Martinelli and Panofsky was:

$$\tau_\pi = (1.97\,^{+0.14}_{-0.17}) \cdot 10^{-8}\text{ sec.} \tag{3}$$

A more precise method for the measurement of the mean life of π-mesons was developed independently by Kraushaar, Thomas, and Henri

(KWL50) and by Chamberlain, Mozley, Steinberger, and Wiegand (CO50). This method is similar, in principle, to that used by Rossi and Nereson and by other experimenters for the determination of the mean life of μ-mesons (§ 4.7).

Figure 1 shows schematically the experimental arrangement used by Kraushaar and his collaborators. A description of the experiment follows, in the words of the authors: "Mesons are produced in a carbon or beryllium target T by γ-rays from the M.I.T. synchrotron. Some of the π-mesons pass through an absorber A_1(0.63 cm Pb + 0.63 cm Al), traverse a 2 g cm^{-2} stilbene crystal X_1 (facing a LP21 photo-multiplier, P_1), a 2 g cm^{-2} bakelite absorber, A_2, and stop in a 1-g cm^{-2} stilbene crystal, X_2 (facing

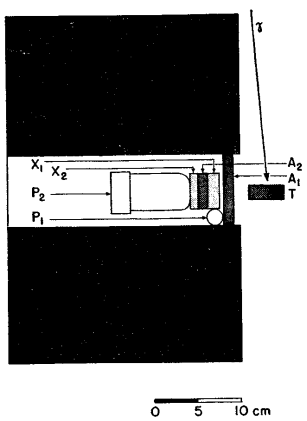

Fig. 4.14.1. Experimental arrangement used by Kraushaar *et al.* for detecting the $\pi \to \mu \to e$ decay by means of scintillation crystals (KWL50). Black areas represent the lead shield.

a 5819 photo-multiplier, P_2). Practically all of the μ-mesons (range 0.1 g cm^{-2}) arising from the decay of the stopped π^+-mesons come to rest in the same crystal, X_2, and subsequently decay, giving rise to positons. The arrival of the π^+-meson, the disintegration of the π^+-meson, and the disintegration of the μ^+-meson produce light flashes that are detected by the photo-multiplier P_2. The resulting pulses are amplified by a distributed constant amplifier, delayed 10^{-7} seconds by a coaxial cable, and displayed on a high writing-speed oscilloscope. The over-all resolution of the crystal and electronic equipment is sufficient to measure the time between arrival and decay of π^+-mesons when this time is $3 \cdot 10^{-8}$ seconds or greater. The pulses from P_2 are also presented on a second slower oscilloscope for the purpose of observing the decay electron from the μ-meson. The sweeps of the two oscilloscopes are triggered simultaneously

by coincidences between P_1 and P_2. The two oscilloscopes are photographed with the same camera on a continually moving film."

In a preliminary set of measurements, Kraushaar and his collaborators selected 57 pictures, each showing a double pulse on the "fast" oscilloscope as well as an additional pulse on the "slow" oscilloscope. They found that the number of these events was consistent with the number of π-mesons stopping in the crystal X_2, as computed from the observed number of mesons ending in the emulsion of a control plate placed near the crystal; they also found that the time distribution of the pulses recorded by the slow oscilloscope was consistent with the known mean life of μ-mesons.

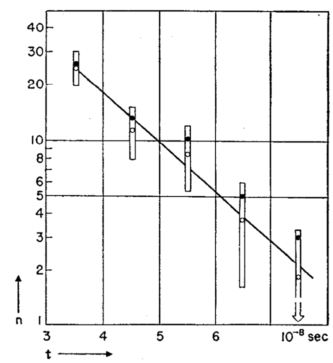

Fig. 4.14.2. Differential decay curve of π^+-mesons obtained by Kraushaar *et al.* The ordinate indicate the numbers, n, of events per 10^{-8} sec time interval. The solid dots are the uncorrected experimental data. The circles are experimental data corrected for accidentals. The straight line corresponds to a mean life at $1.65 \cdot 10^{-8}$ sec. The standard errors indicated are those for the corrected data (KWL50).

There was thus little doubt that the events recorded actually represented $\pi \to \mu \to e$ decay processes. Figure 2 shows the observed distribution of time intervals between the two pulses of the pairs corresponding to $\pi \to \mu$ decays. Both the uncorrected data and those corrected for accidentals are given in this figure. The corrected points give the differential decay curve of positive π-mesons. By fitting an exponential curve to these points, one finds a value of $(1.65 \pm 0.33) \cdot 10^{-8}$ sec. for the mean life.

Chamberlain and his collaborators, using the Berkeley synchrotron as a meson source, made an essentially identical experiment but achieved a much greater statistical accuracy. Their results are shown in Fig. 3 both in the form of a differential and in the form of an integral disintegra-

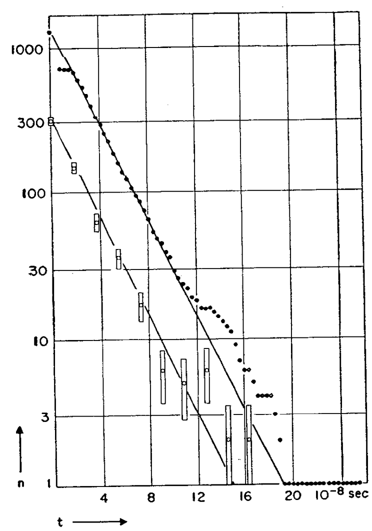

Fig. 4.14.3. The integral decay curve (solid dots) and the differential decay curve of π^+-mesons (open circles) obtained by Chamberlain *et al.* The zero time point on the integral curve represents all observed π-μ decays. The zero time point on the differential curve represents π-μ decays with delays between 2.17 and $3.98 \cdot 10^{-8}$ sec, the next point those with delays between 3.98 and $5.79 \cdot 10^{-8}$ sec, etc. Standard statistical errors for the differential curve are indicated. The straight lines correspond to a mean life of $2.65 \cdot 10^{-8}$ sec (CO50).

tion curve. From the logarithmic slope of these curves one finds the following values for the mean life of positive π-mesons:

$$\tau_\pi = (2.65 \pm 0.12) \cdot 10^{-8} \text{ sec.} \tag{4}$$

Lastly, we wish to mention the preliminary results obtained by Lederman, Booth, Byfield, and Kessler (LLM51), who studied, by means of a cloud chamber, the decay in flight of 90-Mev π^--mesons produced in the Columbia cyclotron. From the number of $\pi \rightarrow \mu$ decays observed and from the total track length of mesons they obtained the following value for the mean life of negative π-mesons:

$$\tau_\pi = (2.92 \pm 0.32) \cdot 10^{-8} \text{ sec.} \tag{5}$$

The results described above make it appear likely that positive and negative π-mesons have the same mean life and that this is close to the

value of $2.65 \cdot 10^{-8}$ sec. measured by Chamberlain and his collaborators. One must probably ascribe to systematic errors the lower values found in earlier experiments.

4.15. ***Neutral π-mesons.*** Since the discovery of charged mesons, the possible existence of neutral mesons has been the subject of many speculations. In 1947, Oppenheimer focused the attention of the physicists upon this problem by suggesting that neutral mesons may be the main source of the electronic component of cosmic rays and, in particular, of the electronic component of extensive air showers [(OJR47); see also (LHW48)].

According to the picture presented by Oppenheimer, nuclear interactions of high-energy particles give rise to comparable numbers of charged and neutral mesons. The latter then disintegrate spontaneously into photons with a very short mean life.

Experiments by means of ionization chambers (BHS47), cloud chambers (FWB48; FWB49.1; CCY49; GPB50), and photographic emulsions (KMF49; CAG50) showed that indeed high-energy photons occur frequently among the products of nuclear interactions of cosmic rays. More definite evidence for the existence of neutral mesons, however, came from experiments with high-energy protons and γ-rays from artificial sources.

Bjorklund, Crandall, Moyer, and York (BR50) at Berkeley were able to detect the production of photons in various targets bombarded with protons of energies ranging from 175 to 350 Mev, and to measure crudely the energy distribution of the photons emitted in different directions. They found that the γ-radiation produced by 175-Mev protons was very weak. Both its intensity and its energy distribution could be explained in terms of an ordinary radiation process (*bremsstrahlung*) of protons. Already at 230 Mev proton energy, however, the photon yield greatly exceeded that predicted for proton bremsstrahlung. This yield continued to increase rapidly with increasing proton energy and at 340 Mev it was about 100 times greater than at 175 Mev. There was thus strong evidence for the production of photons through a process, different from bremsstrahlung, that became effective for proton energies greater than about 175 Mev. Bjorklund and his collaborators tentatively identified this process with the production of neutral mesons (hereafter to be denoted as π^0) immediately followed by their decay into photon pairs:

$$\pi^0 \rightarrow \gamma + \gamma. \tag{1}$$

Measurements on the energy distribution of the photons emitted in different directions provided additional support for the suggested interpretation. This energy distribution was found to be very different from that of γ-rays produced in ordinary radiation processes. The photon intensity, instead of decreasing uniformly with increasing photon energy, rose to a maximum and then decreased again. With a proton beam of

340 Mev energy, the maximum occurred at about 120 Mev for the photons emitted in the direction of the incident protons and at about 60 Mev for the photons emitted in the opposite direction.

Under the neutral-meson hypothesis, the difference in energy between the photons emitted in the two opposite directions is easily explained as a Doppler effect. Indeed it is reasonable to assume that the mesons are produced with an average velocity in the direction of the incident proton beam. From the ratio between the energy of the photons emitted in the forward direction (~120 Mev) and the energy of the photons emitted in the backward direction (~60 Mev) one finds that the velocity of the mesons is about $\frac{1}{3}$ the velocity of light. On the other hand, the total energy of a meson that produces a 120-Mev photon in the forward direction and a 60-Mev photon in the backward direction is $120 + 60 = 180$ Mev. From $\beta = \frac{1}{3}$ and $U = 180$ Mev one computes a value of 170 Mev for the rest energy of the neutral meson. This is only a crude estimate, but it shows that the proposed interpretation does not require an unreasonable value for the mass of the neutral meson.

More recently Steinberger, Panofsky, and Steller (SJ50.2) obtained crucial evidence for the existence of neutral mesons and for the disintegration scheme represented by Eq. (1) with an experiment in which they detected the pairs of photons arising from the decay of individual mesons.

Before discussing this experiment we shall elaborate in some more detail the assumption of the two-photon decay. In the frame of reference of the meson, the two photons are emitted in opposite directions and each has an energy equal to one-half the rest energy of the meson. In the laboratory frame of reference the two photons, in general, have different

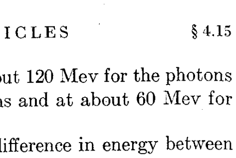

Fig. 4.15.1. Disintegration of a neutral π-meson into two photons of energy E_1 and E_2.

energies. The principles of conservation of energy and momentum yield a simple relation between these energies and the angle enclosed by the trajectories of the photons. Let p represent the momentum of the meson, m_0 its mass; let E_1 and E_2 be the energies of the two photons and θ_1, θ_2 their angles of emission with respect to the trajectory of the meson (Fig. 1). The following equations hold:

$$E_1 \sin\theta_1 - E_2 \sin\theta_2 = 0, \tag{2}$$

$$E_1 \cos\theta_1 + E_2 \cos\theta_2 = cp, \tag{3}$$

$$c^2p^2 + m_0^2c^4 = (E_1 + E_2)^2. \tag{4}$$

From Eqs. (3) and (4) one obtains:

$$m_0^2c^4 = E_1^2 \sin^2\theta_1 + E_2^2 \sin^2\theta_2 + 2E_1E_2 - 2E_1E_2 \cos\theta_1 \cos\theta_2,$$

which, together with Eq. (2) yields:

$$m_0^2c^4 = 2E_1E_2 \sin\theta_1 \sin\theta_2 + 2E_1E_2 - 2E_1E_2 \cos\theta_1 \cos\theta_2,$$

or:

$$\sin\frac{\theta}{2} = \frac{m_0c^2}{2\sqrt{E_1E_2}}, \tag{5}$$

where:

$$\theta = \theta_1 + \theta_2.$$

The angle θ is a minimum when $E_1 = E_2 = U/2$, where U represents the total energy of the neutral meson. For this minimum angle, Eq. (5) yields the following value:

$$\sin\frac{\theta_{min}}{2} = \frac{m_0c^2}{U}. \tag{6}$$

In the frame of reference of the meson, each photon has an energy equal to $m_0c^2/2$ and a momentum equal to $m_0c/2$. Therefore from Eq. (4.13.12) one obtains the following expression for the fractional number of cases in which either one of the two photons has an energy between E_1 and $E_1 + dE_1$ in the laboratory system:

$$dn = \frac{dE_1}{pc}. \tag{7}$$

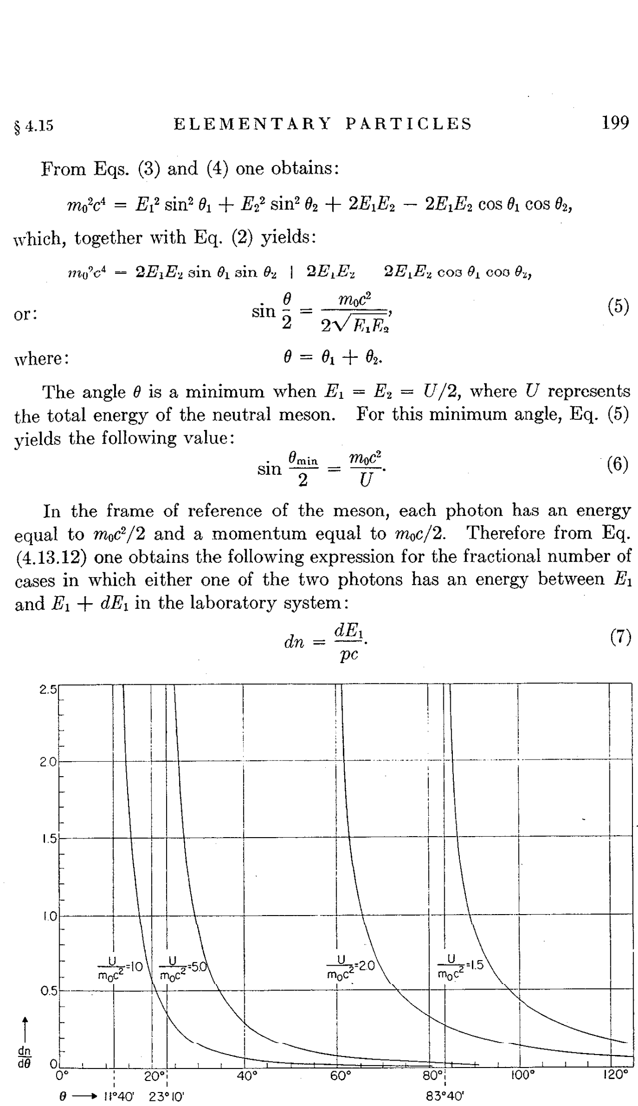

Fig. 4.15.2. The quantity $dn/d\theta$ given by Eq. (4.15.8) plotted as a function of θ for various values of U/m_0c^2. The graphs represent the distribution in angle of the photon pairs produced by the decay of neutral mesons of different total energies, U.

In order to determine the distribution in angle of the pairs, one only needs to combine Eq. (7) with Eq. (5), considering that $E_1 + E_2 = U$. A simple calculation yields the following result:

$$\frac{dn}{d\theta} = \frac{m_0c}{p}\frac{\cos(\theta/2)}{4\sin^2(\theta/2)\sqrt{(U/m_0c^2)^2\sin^2(\theta/2) - 1}}. \tag{8}$$

Equation (8) shows that the distribution function $dn/d\theta$ becomes infinity for $\sin(\theta/2) = m_0c^2/U$, or $\theta = \theta_{\min}$. The graphs in Fig. 2 illustrate the behavior of this function for different values of the energy of the neutral meson. One sees that in all cases most photon pairs are produced with an angle close to the minimum angle defined by Eq. (6).

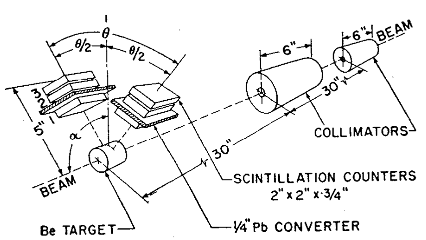

Fig. 4.15.3. Experimental arrangement used by Steinberger *et al.* for the detection of the photon pairs arising from the decay of neutral mesons (SJ50.2).

The experimental arrangement used by Steinberger and his collaborators for the detection of the photon pairs is shown schematically in Fig. 3. Gamma rays from a synchrotron operated at 330 Mev pass through two collimators and then fall upon a beryllium target. Each of the two photon-detectors consist of three scintillation counters, arranged one after the other as shown in the picture, and numbered 1, 2, 3 in order of increasing distance from the target. Lead plates, 0.63 cm thick, are inserted between counters 1 and 2 in each detector. A photon coming from the target and incident upon one of the detectors is likely to traverse counter 1 without interacting and to undergo materialization in the lead, projecting one or both of its secondary electrons through counters 2 and 3. When this happens, counters 2 and 3 will register simultaneous pulses with no pulse recorded by counter 1. If neutral mesons are produced by the synchrotron beam in the target, and if these neutral mesons decay into photon pairs, one will observe coincident pulses of the two pairs of counters 2 and 3 not accompanied by pulses in either of the two counters 1.

Such events were indeed observed. As expected, the counting rate was a sensitive function of the angle, θ, between the axes of the two detectors. With the plane of the axes perpendicular to the γ-ray beam ($\alpha = \pi/2$), the

optimum value of θ was close to 90°. According to Fig. 2, 90° approximately represents the mean angle of the photon pairs produced by the decay of neutral mesons whose kinetic energy is about one-half the rest energy.* This corresponds to a total energy close to 200 Mev, if the rest energy of neutral mesons is close to that of charged π-mesons. Consequently one should expect the mean energy of the observed photons to be approximately 100 Mev.

To test this conclusion, Steinberger and his collaborators changed the thickness and the material of the converters between counters 1 and 2. The corresponding changes of the counting rate were quite consistent with the assumption that the observed events were due to materialization of 100-Mev photons. They also found that lead absorbers, inserted between the target and counters 1, caused the coincidence rate to decrease by a factor consistent with the known absorption coefficient of high-energy photons. Lastly, measurements with aluminum absorbers placed between counters 2 and 3 gave an average range of the secondary electrons close to that of 50-Mev electrons.

Thus the experiment described above shows beyond any reasonable doubt that neutral mesons exist, that their mass is close to that of the charged π-mesons, and that the decay of each neutral meson gives rise to two photons, according to Eq. (1).

Photons have spin 1 and therefore Eq. (1) shows that neutral mesons have either spin 0, in which case the two photons arising from the decay of each meson have anti-parallel spins, or spin 2, in which case the photons have parallel spins. The existence of an elementary particle with spin 2 seems to be only a very remote possibility and we thus conclude that *neutral π-mesons have almost certainly spin zero.*

There appears to be an intimate relationship between neutral mesons and charged π-mesons. Indeed, both kinds of mesons are produced directly and with comparable abundance in nuclear interactions. Also, their masses are very similar (§ 4.16). Thus the fact that neutral mesons have spin zero gives indirect support to the assumption that the spin of charged π-mesons is also zero, rather than one.

The mean life of neutral mesons, τ_0, has not yet been determined. However, one can place an upper limit to its value. In an experiment performed with the 184-inch Berkeley cyclotron, neutral mesons were produced in a 0.0025-cm wolfram wire placed in the circulating 380-Mev proton beam and the photons arising from their decay were observed by means of a pair-detector. A uranium block was inserted gradually be-

* It is hardly necessary to point out that, even if the π^0-mesons were monoenergetic, the function describing the dependence of the counting rate on the angle, θ, between the axes of the telescopes would not coincide with the distribution function, $dn/d\theta$, given by Eq. (8). The latter represents the distribution per unit plane angle. The former, instead, gives the distribution per unit solid angle, further modified by the geometry of the instrument.

tween the source and the detector. The shadow cast by this block was found to be very sharp, indicating that the source of photons did not have dimensions appreciably greater than the target where the neutral mesons originated. It was thus possible to conclude that the neutral mesons did not travel, on the average, a distance greater than about 0.0025 cm before disintegrating. If one recalls the expression for the mean distance before decay Eq. (4.7.1), and considers that the average momentum of the neutral mesons produced by 380-Mev protons is of the order of m_0c, one obtains from this experiment an upper limit of the order of 10^{-13} sec for the mean life of neutral mesons.*

Observations on high-energy photons associated with nuclear interactions of cosmic rays lead to a similar conclusion. These photons, assumed to be the decay products of neutral mesons, reveal their existence by producing electron pairs or by initiating showers. From the average distance between the point where the nuclear interaction occurs and the point where photons manifest themselves one can estimate an upper limit for the mean life of neutral mesons. In this way Bradt, Kaplon, and Peters (BHL50.3) found $\tau_0 < 10^{-13}$ sec and Gregory and Tinlot (GBP51) found $\tau_0 < 10^{-12}$ sec.

In a recent paper, Carlson, Hooper, and King (CAG50) pointed out that one can obtain more precise information on the mean life of neutral mesons through a careful study of electron pairs appearing in photographic emulsions near the point of origin of high-energy nuclear interactions. The trajectory of the photon responsible for a given electron pair is intermediate between the trajectories of the two electrons of the pair. Therefore the bisector of the angle between the tracks of the two electrons determines the direction of motion of the parent photon with an error not greater than half the angular aperture of the pair. If the photons are produced by the decay of neutral mesons of finite mean life, the lines of flight of the photons will pass some distance from the origin of the nuclear interactions. From the mean value of this distance one can obtain an estimate of the meson mean life.

The method described above is considered capable of measuring mean lives as short as $2 \cdot 10^{-14}$ seconds. Preliminary results indicate that the mean life of neutral mesons is not much greater than this value and is probably shorter than $5 \cdot 10^{-14}$ sec. Indeed, the authors quote a figure of $3 \cdot 10^{-14}$ sec. as the most likely value for the mean life of π^0-mesons.

4.16. *Capture of π^--mesons by protons and deuterons.* We have already mentioned in § 4.12 that a free proton cannot capture a negative π-meson and change into a neutron without at least another particle being produced. The presence of this particle (or particles) is required by the conservation laws of energy and momentum. If only one additional

* Reported by H. York at the April 1950 meeting of the American Physical Society in Washington.

particle is produced, it must have integer spin. It could thus be a photon or, as suggested by Marshak and Wightam (MRE49), a neutral π-meson which then disintegrates into a pair of photons. Symbolically, the two processes are:

$$p + \pi^- \rightarrow n + \gamma, \tag{1}$$

$$p + \pi^- \rightarrow n + \pi^0 \rightarrow n + \gamma + \gamma. \tag{2}$$

The total energy released in each process equals the rest energy of the charged π-meson ($m_\pi c^2 = 141$ Mev; § 4.13), minus the difference between the rest energies of the neutron and the proton ($\Delta = 1.3$ Mev; § 4.4):

$$m_\pi c^2 - \Delta \approx 140 \text{ Mev}. \tag{3}$$

In a process of the first kind, this energy is subdivided among a photon and a neutron, in such a manner that the two particles acquire equal (and opposite) momenta. If E_γ is the energy of the photon, E_n the kinetic energy of the neutron, and M_n the mass of the neutron, the two following equations hold:

$$E_\gamma + E_n = m_\pi c^2 - \Delta, \tag{4}$$

$$\frac{E_\gamma}{c} = \sqrt{2M_nE_n}, \tag{5}$$

where $\sqrt{2M_nE_n}$ represents the momentum of the neutron in the nonrelativistic approximation. From these two equations one obtains:

$$E_\gamma \approx 131 \text{ Mev}, \qquad E_n \approx 9 \text{ Mev}. \tag{6}$$

Thus most of the available energy goes into the photon. A process of the second kind can take place only if the neutral meson is lighter than the charged meson and if the difference between the rest energies of these two particles:

$$\delta = m_\pi c^2 - m_0 c^2 \tag{7}$$

is equal or greater than the difference, Δ, between the rest energies of the proton and neutron.

If $\delta = \Delta$, the π^0-mesons are produced at rest and the photons arising from their decay have all the same energy, equal to $m_0c^2/2$, or approximately 70 Mev.

If $\delta > \Delta$, the π^0-mesons are produced with a kinetic energy E_0 given by the equations:

$$E_0 + E_n = \delta - \Delta, \tag{8}$$

$$\sqrt{2M_nE_n} = \sqrt{2m_0E_0}, \tag{9}$$

where it has been assumed that $E_0 \ll m_0c^2$ so that the momentum of the π^0-meson, as well as that of the neutron, can be expressed by means of the nonrelativistic approximation. From Eqs. (8) and (9) one obtains:

$$E_0 = \frac{\delta - \Delta}{1 + \frac{m_0}{M_n}}. \tag{10}$$

The neutral mesons are produced at random in direction. Therefore the intensity as well as the energy distribution of the photons arising from their decay are the same in all directions. The energy spectrum of the photons observed in *any given direction* is thus identical to the energy spectrum of the photons emitted by a parallel beam of π^0-mesons of kinetic energy E_0, *averaged over all directions*. From the considerations developed in § 4.13 it follows that if $E_0 \ll m_0c^2$, the minimum and maximum energies of these photons are:

$$E_{\min} = \frac{(m_0c^2 + E_0)}{2} - \sqrt{\frac{E_0m_0c^2}{2}},$$
$$E_{\max} = \frac{(m_0c^2 + E_0)}{2} + \sqrt{\frac{E_0m_0c^2}{2}}. \tag{11}$$

It also follows that the energy spectrum of the photons is flat between the two limits $E_{\min}$ and $E_{\max}$. Equations (11) yield the following expression for the energy spread of the photons:

$$E_{\max} - E_{\min} = \sqrt{2E_0m_0c^2}. \tag{12}$$

Theoretical arguments indicate that when a π^--meson is captured into a Bohr orbit of a proton, the probability for the occurrence of process (1) or process (2) (if the latter is energetically possible) is much greater than the probability for spontaneous decay. Regardless of whether π^--mesons disappear through process (1) or process (2), one should expect γ-ray emission to follow the absorption of negative π-mesons in hydrogen.

This effect has been demonstrated experimentally by Panofsky and his collaborators (PWK50.1; PWK50.3; PWK51). Figure 1 shows the arrangement used in the latest experiments of those authors. 330-Mev protons in the internal beam of the 184-inch Berkeley cyclotron strike a wolfram target. Some of the negative π-mesons produced in the interactions of the protons with the wolfram nuclei come to rest within a high-pressure tank of hydrogen gas (H_2) placed close to the target. The γ-rays arising from the capture of these mesons are analyzed by means of a pair spectrometer.

Materialization of the photons takes place in a tantalum foil (Ta). The positive and negative electrons arising from each materialization process are deflected in opposite directions by a magnetic field (from 5,000 to 10,000 gauss) perpendicular to the plane of the drawing. If these electrons have energies within appropriate limits, they may pass through the proportional counters P_1, P_2, P_3, P_4, giving rise to a fourfold coincidence. The fourfold coincidence activates a register recording the pulses

of 32 individual Geiger-Mueller counters arranged in two trays, C_1 and C_2. From the record one can discover which pair of Geiger-Mueller counters has been discharged by the two electrons arising from each materialization process and can thus determine the energies of these electrons within narrow limits.

Preliminary results obtained by Panofsky and his collaborators showed that the photons emanating from the hydrogen tank were not monoenergetic (PWK50.1). There appeared to be a group of photons of about 70 Mev energy and another group of about 130 Mev energy, although the poor resolution of the instrument did not afford a sharp separation of the two groups.

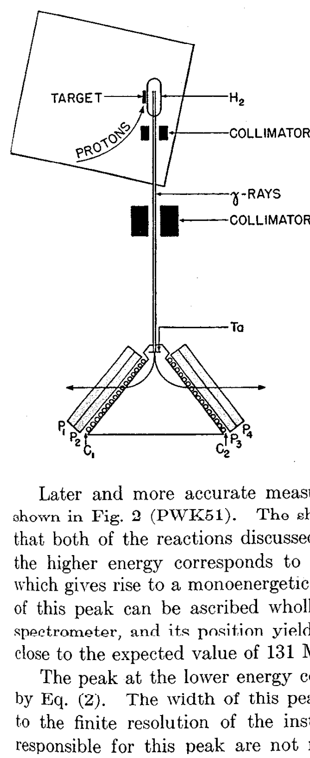

Fig. 4.16.1. Experimental arrangement used by Panofsky *et al.* for the detection of photons arising from the absorption of negative π-mesons in hydrogen (PWK51).

Later and more accurate measurements yielded the γ-ray spectrum shown in Fig. 2 (PWK51). The shape of this spectrum clearly indicates that both of the reactions discussed above actually occur. The peak at the higher energy corresponds to the reaction represented by Eq. (1), which gives rise to a monoenergetic group of photons. Indeed, the width of this peak can be ascribed wholly to the finite resolution of the pair spectrometer, and its position yields for the photon energy a value very close to the expected value of 131 Mev.

The peak at the lower energy corresponds to the reaction represented by Eq. (2). The width of this peak is somewhat greater than that due to the finite resolution of the instrument, indicating that the photons responsible for this peak are not monoenergetic. It thus appears that the neutral mesons arising from the capture of π^--mesons in hydrogen have a finite kinetic energy. The experimental data are consistent with a constant distribution of photons between the limits $E_{min} = 54$ Mev and

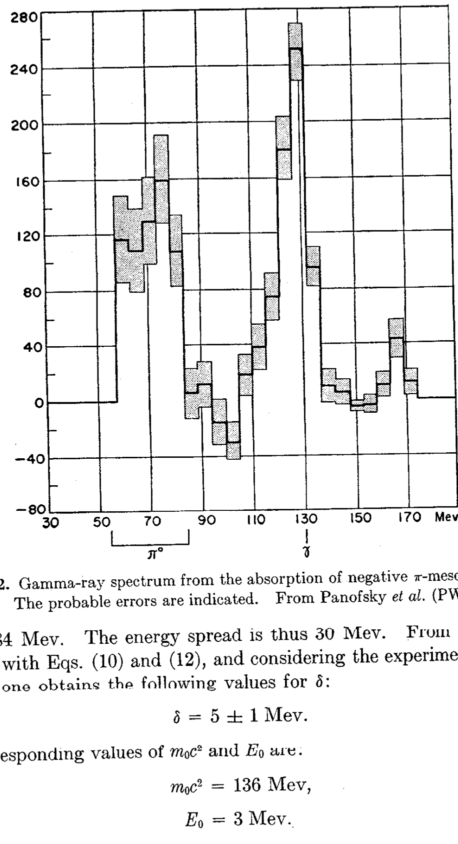

Fig. 4.16.2. Gamma-ray spectrum from the absorption of negative π-mesons in hydrogen. The probable errors are indicated. From Panofsky *et al.* (PWK51).

$E_{max} = 84$ Mev. The energy spread is thus 30 Mev. From this result, together with Eqs. (10) and (12), and considering the experimental uncertainties, one obtains the following values for δ:

$$\delta = 5 \pm 1 \text{ Mev.} \tag{13}$$

The corresponding values of m_0c^2 and E_0 are:

$$m_0c^2 = 136 \text{ Mev,} \tag{14}$$

$$E_0 = 3 \text{ Mev.} \tag{15}$$

From these values and from Eqs. (11) one obtains:

$$E_{\min} + E_{\max} = m_0c^2 + E_0 = 139 \text{ Mev,}$$

in agreement with the assumed values of $E_{\min}$ and $E_{\max}$. This checks the internal consistency of the analysis.

Note that the width of the photon distribution is a very sensitive function of δ, so that a crude knowledge of $E_{\max} - E_{\min}$ suffices to establish the mass of the neutral meson quite accurately.

By measuring the areas under the two peaks and considering that two photons are emitted by the decay of each π^0-meson, one can determine the ratio of the probabilities for the two competing processes represented by Eqs. (1) and (2). The experimental value of this ratio turns out to be very close to one.

It is interesting to note that experiments performed with hydrogenous compounds (polyethylene, lithium hydride) in place of pure hydrogen failed to reveal any detectable γ-radiation (PWK50.1). Presumably the reason is that the π^--mesons are initially captured by the hydrogen nuclei into highly excited Bohr orbits. The neutral systems thus formed diffuse through the lattice and make many collisions with the heavier nuclei of the compound before the π^--mesons can fall into Bohr orbits sufficiently close to the proton for the meson-proton reaction to occur. During these collisions the π^--meson has a large probability of being captured by one of the heavier nuclei, with consequent production of a nuclear star (PWK50.1).

With the experimental arrangement described in Fig. 1, Panofsky and his collaborators investigated also the stopping of negative π-mesons in deuterium gas (PWK50.4; PWK51). They found that this process is accompanied by the emission of a continuous spectrum of γ-rays, extending to an energy close to the rest-energy of π-mesons, and with a sharp maximum near the upper end. This result shows that the absorption of π^--mesons by deuterons occurs, at least partially, according to the reaction:

$$d + \pi^- \rightarrow n + n + \gamma. \tag{16}$$

The γ-ray spectrum does not exhibit a secondary maximum at about $m_\pi c^2/2$, and one must thus conclude that the reaction

$$d + \pi^- \rightarrow n + n + \pi^0 \rightarrow n + n + \gamma + \gamma \tag{17}$$

either does not occur or is much less frequent than the reaction (16).

However, a comparison between the γ-ray intensities observed with hydrogen and with deuterium, respectively, indicates that only 30 per cent of the absorption processes occur according to (16). The remaining 70 per cent of the events do not give rise to γ-rays and correspond presumably to the reaction:

$$d + \pi^- \rightarrow n + n. \tag{18}$$

As already pointed out in 4.9, the nonradiative capture of π^--mesons is practically the only type of absorption process occurring in heavier nuclei.

4.17. ***New unstable particles.*** Various observers have described observations suggesting the existence of unstable particles different from those considered thus far in this chapter.

L. Leprince-Ringuet (LRL44) obtained a mass value of 990 from application of the principles of conservation of energy and momentum to a cloud chamber picture of a collision of a positive particle with an electron.

Brown and her collaborators (BRH49.2), working with electron-sensitive emulsions, reported the observation of a particle with apparent mass near 1000 electron masses, that came to rest in the emulsion. From the end of its trajectory, three particles seemed to originate, all of which were certainly heavier than electrons and probably lighter than protons. One of them could be identified as a π^--meson because it gave rise to a star after stopping in the emulsion. The trajectories of the three secondary particles were coplanar within the experimental uncertainty. This event and two similar events reported by Harding (HJB50) were tentatively interpreted as the decay of positive "heavy" mesons (τ-mesons) into groups of 3 π-mesons.

Leprince-Ringuet (LRL49.1) observed what might have been a negative "heavy" meson; i.e., a particle that, after coming to rest in the emulsion, seemed to undergo nuclear absorption and to produce a star of such a character as to require an energy release of at least 700 times the electron rest energy. An event of similar type was reported by Forster (FHH50.1).

In a series of experiments performed at 3250 meters above sea level, Alichanian and his collaborators (AAI48) selected cosmic-ray particles with different ranges in lead and measured their magnetic deflection. They used a large number of Geiger-Mueller counters arranged in different layers above and below the magnet to study the trajectories of the particles. From their experimental results they concluded that mesons of many different masses exist. To these mesons they gave the name of "varitrons." Despite the confirming evidence from observations in photographic plates reported by workers of the same group (AAI49), the interpretation of the experiment described above appears incorrect, especially in view of the results of Brode and his collaborators described in § 4.11.

Perhaps the most convincing evidence for the existence of new kinds of particles comes from the cloud chamber observations of the so-called "V-tracks." These tracks are interpreted as showing either the decay of neutral particles (V^0-particles) into pairs of positive and negative particles, or the decay of charged particles ($V^{\pm}$-particles) into pairs of charged and neutral particles.

The first observations of this kind were reported by Rochester and Butler (RGD47.1), who obtained the two pictures reproduced in Figs. 1 and 2 with a magnet cloud chamber operated at sea level. In the first picture one sees two ionizing particles, a and b, the first positive, the second negative, diverging at a wide angle from a point in the gas a short distance

Fig. 4.17.1 (opposite page). Cloud-chamber pictures obtained by Rochester and Butler (RGD47.1), interpreted as showing the decay in flight of V-particles. (1) A neutral V-particle decays into two charged particles (a) and (b). (2) A charged V-particle (a) decays into a charged particle (b) and a neutral particle.

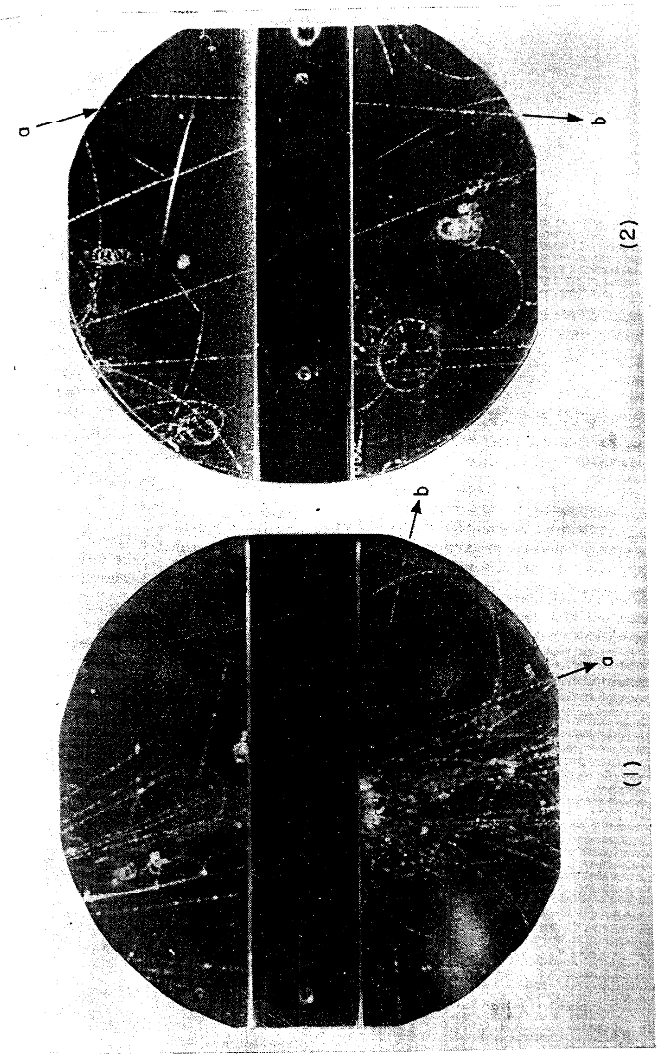

below a 3-cm lead plate placed across the chamber. Supposedly these two particles are the two charged products of the decay of a neutral V-particle. In the second picture one sees an ionizing positive particle entering the chamber from above (track a) and undergoing a sudden large-angle deflection in the gas; the deflected particle (track b) goes through the lead plate without producing secondary effects and undergoing only a small amount of scattering. Supposedly track a represents a positive V-particle and track b represents its charged disintegration product. Note that in both pictures the V-particle appears simultaneously with penetrating particles from nuclear interactions occurring above the chamber.

In 1950 Anderson and his collaborators (SAJ50) reported the observation of 30 additional pictures of the first type (Fig. 1) and of four additional pictures of the second type (Fig. 2). These pictures were obtained partly at sea level, partly at 3,200 meters altitude with a magnet cloud chamber containing a 2-cm lead plate and triggered by an arrangement of counters selecting penetrating showers. More recently, Bridge, Harris, and Rossi (BHS51.1), Fretter (FWB51.1), and Armenteros, Barker, Butler, Cachon, and Chapman (AR51) obtained further evidence of the neutral and charged V-particles.

The following arguments show that the V-tracks represent spontaneous disintegration processes rather than collision processes. Firstly, the probability for their occurrence appears to depend on the distance traveled and not on the amount of matter traversed. If it were not so, for each event occurring in the gas one should observe hundreds of events occurring in the metal plates contained in the chamber. The results of Rochester and Butler as well as those of the other experimenters, definitely show that this is not the case, even if one considers that events occurring in a solid plate are more difficult to recognize than those occurring in the gas. Secondly, if one tries to interpret the events of the second type (Fig. 2) as scattering processes due to collisions with nuclei, one finds that in most cases the nucleus should have received sufficient momentum to produce a short but detectable track. No such recoil appeared in any picture.

With regard to the nature of the charged secondary particles, the following information is available. (a) These particles are singly charged, as shown by their specific ionization. (b) They are heavier than electrons, because none of those that went through lead plates appeared to produce cascade showers. (c) Some of the particles arising from the decay of V^0-particles are lighter than protons; some, however, seem to have protonic mass (AR51). (d) In some cases, one of the charged particles arising from the decay of a V^0-particle appears to undergo nuclear scattering on traversing a metal plate (SAJ50; AR51). In one case the charged particle arising from the decay of a charged V-particle undergoes nuclear scattering in an aluminum plate, traverses several other lead and aluminum plates, and then comes to rest in the chamber (BHS51; see Fig. 8.1.21). From ionization and scattering, the particle manifests itself as a meson. Since μ-mesons do not interact with nuclei appreciably, it must be a π-meson.

There is no direct information as yet concerning the nature of the neutral particle that must be produced simultaneously with the charged particle by the decay of a $V^{\pm}$-particle.

The available experimental data are not sufficient to determine the mode of disintegration of the V-particles, nor to establish their identity. Among the disintegration schemes that have been suggested are the following:

$$V^0 \to \pi^+ + \pi^- \quad (1); \qquad V^{\pm} \to \pi^0 + \pi^{\pm} \quad (1').$$

$$V^0 \to p + \pi^- \quad (2); \qquad V^{\pm} \to n + \pi^{\pm} \quad (2').$$

Scheme (1) would not explain the presence of protons among the disintegration products of V^0-particles. On the other hand, the observations of Armenteros and his collaborators (AR51) have shown that occasionally π^+-mesons are produced by the decay of V^0-particles. This effect cannot be accounted for by scheme (2).

Of course, there may be more than one kind of neutral and charged V-particles. Also, one must consider the possibility that, in some cases at least, the disintegration may give rise to more than two secondary particles (e.g., $V^0 \to n + \pi^+ + \pi^-$).

In the pictures showing the decay of neutral V-particles (Fig. 1), one can measure the angle, θ, between the trajectories of the two secondary particles. Let m_1 and m_2 be the masses of the secondary particles. Let m_V be the mass and p_V the momentum of the primary particle. Under the assumption of a two-body disintegration, the conservation laws of energy and momentum yield the following equations:

$$\left.\begin{aligned} p_1^2 + p_2^2 + 2p_1p_2\cos\theta &= p_V^2, \\ \sqrt{c^2p_1^2 + m_1^2c^4} + \sqrt{c^2p_2^2 + m_2^2c^4} &= \sqrt{c^2p_V^2 + m_V^2c^4}. \end{aligned}\right\} \quad (1)$$

Elimination of p_V yields a relation between p_1, p_2, m_1, m_2, m_V.

Similarly, in the pictures showing the decay of charged V-particles (Fig. 2) one can measure the angle, θ_1, between the trajectory of the primary particle and that of the secondary charged particle. The conservation principles then yield the two following equations:

$$\left.\begin{aligned} p_V^2 + p_1^2 - 2p_Vp_1\cos\theta_1 &= p_2^2, \\ \sqrt{c^2p_V^2 + m_V^2c^4} - \sqrt{c^2p_1^2 + m_1^2c^4} &= \sqrt{c^2p_2^2 + m_2^2c^4}, \end{aligned}\right\} \quad (2)$$

where the index 2 refers to the neutral disintegration product. Elimination of p_2 gives a relation between p_V, p_1, m_V, m_1, m_2.

Thus in both cases one can determine the mass, m_V, of the V-particle if one knows the masses, m_1 and m_2, of the two disintegration products and if one measures the momentum (or any other energy-dependent parameter) on each of the two "visible" branches of the V-track.

The values of m_V determined in this manner are of the order of 1000 electron masses for V-particles disintegrating according to (1) and of the order of 2200 electron masses for V-particles disintegrating according to (2).

Anderson and his collaborators attempted to estimate the mean life of V-particles by observing the distribution of the decay points along the lines of flight. For the neutral V-particles, they arrived at a tentative value of $(3 \pm 2) \cdot 10^{-10}$ sec. The charged V-particles appeared to have a somewhat shorter mean life.*

4.18. *Mesons and nuclear forces.* Several years before the discovery of mesons in cosmic rays, Yukawa predicted, on theoretical grounds, the existence of particles with mass intermediate between those of the electron and proton (YuH35). Crudely, the argument leading to this prediction may be described as follows:

The attraction and repulsion between electrically charged particles is a consequence of the electromagnetic field that originates from the charges and, in turn, acts upon the charges. Application of quantum laws to the electromagnetic field leads to the conclusion that its energy is subdivided into discrete quanta. The equations that give the probability of detecting one of these quanta at a given time and in a given region of space coincide with those describing the motion of a particle with zero rest mass in the language of quantum mechanics. Thus the existence of an electromagnetic field, together with the general laws of quantum theory, necessarily implies the existence of particles with zero mass. These particles, of course, are the well known "photons."

Nuclei are held together by forces different from electromagnetic forces. One of the main features of nuclear forces is that they act only at very short distances (of the order of 10^{-13} cm). If one tries to describe these short-range forces in the frame of field theory, one obtains again equations that imply the existence of particle-like radiation quanta. However, the quanta corresponding to the nuclear field, or "Yukawa particles," unlike those corresponding to the electromagnetic field, have a finite mass, m. Between this mass and the range of nuclear forces, R, there exists the following relation:

$$R \approx \frac{\hbar}{mc}. \qquad (1)$$

From the experimental value of R one obtains for m a value of about 300 electron masses.

It is not completely sure that the Yukawa particle coincides with any of the experimentally known mesons. If it does, however, it must be

* More recent results on V-particles (which do not alter essentially the picture presented above) are contained in refs. (BHS51.2), (TRW51), (LRB51), and (FWB51.2).

identified with the π-meson, not with the μ-meson. In the first place, Yukawa particles must be produced by the direct interaction between two nucleons, the way that photons are produced by the interaction between charged particles. Experiments indicate that π-mesons are the direct products of nuclear collisions of protons or neutrons, whereas μ-mesons appear to originate from the spontaneous decay of π-mesons. Also, Yukawa particles must interact strongly with nucleons, the way that photons interact strongly with electrically charged particles (photoeffect, Compton effect, pair production). The experimental finding that the mean life before nuclear capture is much smaller for negative π-mesons at rest than for negative μ-mesons at rest is a proof that nuclear interactions of π-mesons are much stronger than nuclear interactions of μ-mesons. Lastly one may also mention that the mass of the Yukawa particle, as derived from Eq. (1), comes closer to the mass of the π-meson than to the mass of the μ-meson.

From a historical point of view, it is interesting to note that Yukawa also predicted, on theoretical grounds, the instability of mesons. Even though the theoretical arguments leading to this prediction appear questionable in the light of our present knowledge, it is nevertheless true that Yukawa's prediction was largely responsible for the experimental discovery of the μ-meson decay.